CONSTRUCTION AND PRELIMINARY TEST OF A TRAVERSING STAGNATION PRESSURE PROBE FOR A LARGE SCALE AEROTHERMOPRESSOR

James Wilber Carpenter
and
William Leicester Martin III

CONSTRUCTION AND PRELIMINARY TEST OF A TRAVERSING

STAGNATION PRESSURE PROB A LARGE SCALE

JAMES WILBU GRADE, U.S. NAVY

WILLIAM LEICESTER GRADE, U.S. Navy

B.S.

SUBMI

OF

8854
on spine:

CARPENTER

1954

THESIS
C267

Letter on front cover:

CONSTRUCTION AND PRELIMINARY
TEST OF A TRAVERSING STAGNATION
PRESSURE PROBE FOR A LARGE SCALE
AEROTHERMOPRESSOR

James Wilbur Carpenter
and
William Leicester Martin III

CONSTRUCTION AND PRELIMINARY TEST OF A TRAVERSING

STAGNATION PRESSURE PROB A LARGE SCALE

AER

8854

on spine: CARPENTER

1954

THESIS
C267

Letter on front cover:

CONSTRUCTION AND PRELIMINARY
TEST OF A TRAVERSING STAGNATION
PRESSURE PROBE FOR A LARGE SCALE
AEROTHERMOPRESSOR

James Wilbur Carpenter
and
William Leicester Martin III

AND PRELIMINARY TEST OF A TRAVERSING
N PRESSURE PROBE FOR A LARGE SCALE
AEROTHERMOPRESSOR

by

JAMES WILBUR CARPENTER, LIEUTENANT JUNIOR GRADE, U.S. NAVY
B.S., U.S. Naval Academy (1949)

and

WILLIAM LEICESTER MARTIN III, LIEUTENANT JUNIOR GRADE, U.S. Navy
B.S., U.S. Naval Academy (1949)

SUBMITTED IN PARTIAL FULFILLMENT
OF THE REQUIREMENTS FOR THE
DEGREE OF NAVAL ENGINEER

at the
MASSACHUSETTS INSTITUTE OF TECHNOLOGY

Cambridge, Massachusetts
May 24, 1954

Professor Leicester F. Hamilton
Secretary of the Faculty
Massachusetts Institute of Technology
Cambridge 39, Massachusetts

Dear Sir:

In accordance with the requirements of the degree of Naval Engineer, we herewith submit a thesis entitled "Construction and Preliminary Test of a Traversing Stagnation Pressure Probe for A Large Scale Aerothermopressor".

Respectfully,

ABSTRACT

CONSTRUCTION AND PRELIMINARY TEST OF A TRAVERSING STAGNATION PRESSURE PROBE FOR A LARGE SCALE AEROTHERMOPRESSOR

by

JAMES W. CARPENTER, LIEUTENANT JUNIOR GRADE, U.S. NAVY

and

WILLIAM L. MARTIN III, LIEUTENANT JUNIOR GRADE, U.S. NAVY

Submitted to the Department of Naval Architecture and Marine Engineering on May 24, 1954, in partial fulfillment of the requirements for the degree of Naval Engineer.

The objective of this thesis was to construct and test a probe for measuring the gas stagnation pressure of a high speed, moisture-laden gas stream, with a suitable traversing mechanism for use with a large scale aerothermopressor.

Two basically identical probes satisfying the criteria as determined by Dussourd (3) have been constructed and were tested. Two traversing mechanisms were constructed for these probes. One employs a lead screw and universal joint, geared drive with a counter to determine the position of the probe within the duct. The other arrangement merely provides support for the probe and traversing is done by hand with the probe position determined by a direct reading pointer and scale.

It has been determined that the maximum spread in the measurements obtained by these probes is three percent and it is therefore concluded that these probes will give satisfactory measurements of stagnation pressure in the large scale aerothermopressor. It is recommended that the relative merits of the two traversing mechanisms be evaluated from the viewpoints of economics and convenience in the large scale aerothermopressor.

Thesis Supervisor: A. H. Shapiro
Title: Professor of Mechanical Engineering

Table of Contents

I. Introduction 1

II. Procedure 3

- A. Probe Construction 3
- B. Probe Test 4
- C. Traversing Mechanism Construction 6

III. Results 9

IV. Discussion Of Results 18

- A. Probe Measurements 18
- B. Probe Strength 25
- C. Traversing Mechanism 26

V. Conclusions 27

VI. Recommendations 28

VII. Appendix 29

- A-1 List of Symbols Used in Text 30
- A-2 Details of Procedure 33
- B-1 Probe Strength Calculations 35
- B-2 Sample of Primary Data Point Calculations .. 47
- B-3 Sample of Modified Data Point Calculations . 48
- C-1 Summary of Dry Run Calculations 53
- C-2 Summary of Probe Error Calculations for Normal Air 55
- C-3 Summary of Primary Data Point Calculations . 56
- C-4 Summary of Modified Data Point Calculations. 59
- D Original Data 61
- E Literature Citations 67

List of Figures and Tables

Figures

I. Gas Stagnation Pressure Probe 5

II. Small Scale Test Equipment 7

III. Probe Traversing Mechanism 10

IV. Non-Dimensionalized, Stagnation Pressure vs. Static Pressure 11

V. Non-Dimensionalized, Stagnation Pressure vs. Static Pressure 12

VI. Probe Error in Normal Air 13

VII. Stagnation-Static Pressure Ratio - Test II 14

VIII. Stagnation-Static Pressure Ratio - Test III 15

IX. Stagnation-Static Pressure Ratio - Test IV. 16

X. Stagnation-Static Pressure Ratio - Test V 17

XI. Differential Static Pressure vs. Distance Along Test Section 32

XII. Drag Coefficient vs. Mach Number 43

XIII. Maximum Stress vs. Mach Number 45

XIV. Strength Properties of Stainless Steel(Type 304) 46

XV. Differential Static Pressure vs. Differential Stagnation Pressure - Test II 49

XVI. Differential Static Pressure vs. Differential Stagnation Pressure - Test III 5

XVII. Differential Static Pressure vs. Differential Stagnation Pressure - Test IV 51

XVIII. Differential Static Pressure vs. Differential Stagnation Pressure - Test V 52

Tables

I. Summary of Maximum Stress Calculations 44

II. Summary of Dry Run Calculations 53

III. Summary of Probe Error Calculations for Normal Air 55

IV. Summary Primary Data Point Calculations 56

V. Summary of Modified Data Point Calculations 59

VI. Original Data 61

I. Introduction

The objective of this thesis is to construct and test a stagnation pressure probe with suitable traversing mechanism for use with a large scale aerothermopressor. (The aerothermopressor is a device in which atomized water is introduced into a hot, high-speed gas stream, with the aim of realizing the rise in stagnation pressure which gas dynamics indicates as being possible when the stagnation temperature of a high-speed gas stream is reduced (1)).

It has been determined that the experimental performance of an aerothermopressor can be correlated more effectively with a theoretical analysis of the aerothermopressor process (2) if the gas stagnation pressure in this device can be measured. The probe to be constructed, therefore, must be capable of measuring the gas stagnation pressure of a high-speed, droplet-laden gas stream. (By definition, the gas stagnation pressure is the theoretical pressure which would be obtained if the gas phase alone could be decelerated reversibly to zero velocity without momentum interchange or heat transfer between the gas phase and the water droplets).

Most of the theoretical analysis of the aerothermopressor process to date has been one-dimensional in nature. Since the fluid flow in an actual aerothermopressor is a type of pipe flow, it is expected that at any point along the axis of flow, the fluid properties will be a function of the radius of the pipe. Consequently, proper interpre-

tation of the experimental data for comparison with the one-dimensional theoretical analysis requires that a radial traverse of the fluid properties be taken. It would be advantageous also to have an axial traverse; however, mechanical difficulties preclude the latter type of arrangement at this stage of the development. For these reasons the traversing mechanism has been designed to take radial traverses at nine-inch intervals along the flow axis.

II. Procedure

A. Probe Construction

In order to accomplish its intended purpose, this probe must have two distinctive features not found on the ordinary stagnation pressure measuring instrument. First, some means must be employed to drain the water from the probe, and secondly, the nose of the probe must be so designed as to minimize the distortion of the streamlines at the probe tip so as to reduce the effect of momentum exchange between the water droplets and the gas stream.

The geometry of a probe which satisfies these requirements has been determined by Dussourd (3). He found that if the probe is constructed open at both ends, the water which enters the probe will drain satisfactorily, and the accuracy of the stagnation pressure measurement will be unaffected provided the ratio of exit to entrance areas is approximately 0.05. In order to minimize the effect of momentum interchange at the probe tip, the ratio of inside to outside diameters of the probe tip must be unity; however, from the standpoint of construction this is not feasible. Dussourd determined that in order for a probe to be sufficiently accurate, this ratio must not be less than 0.75.

Two basically identical probes satisfying the above criteria have been constructed, the details of which are shown in figure I. Their stems have been individually designed to operate in two different traversing mechanisms.

The probes were manufactured of type 304 stainless steel joined with high temperature silver brazing to permit operation in the large scale aerothermopressor at temperatures up to fifteen hundred degrees Fahrenheit. That part of the probe stem which will extend into the gas stream is of airfoil cross-section to reduce the drag force and to provide adequate strength. Strength calculations will be found in appendix B-1. The probe stem was placed seven diameters from the tip of the probe to reduce the stem's distortion of the streamlines in the vicinity of the probe tip.

B. Probe Test

The testing of these probes was carried out in equipment designed by Wadleigh (4) and constructed under the sponsorship of the aerothermopressor project. This apparatus consists of a converging nozzle and constant area, two and one-eighth inch diameter test section constructed of transparent lucite. There is an atmospheric inlet to the subsonic nozzle and flow is maintained by an exhaust vacuum created by the gas turbine laboratory steam ejector. Water is injected into the air stream by probe number six of table one of reference (4) (see figure II). The probes were inserted in the last testing port, which is located just upstream of the diffuser.

The performance of the probes was checked by comparison with data for similar flow conditions obtained from the experiments of Dussourd. To establish similar flow conditions,

FIGURE I
GAS STAGNATION PRESSURE PROBE

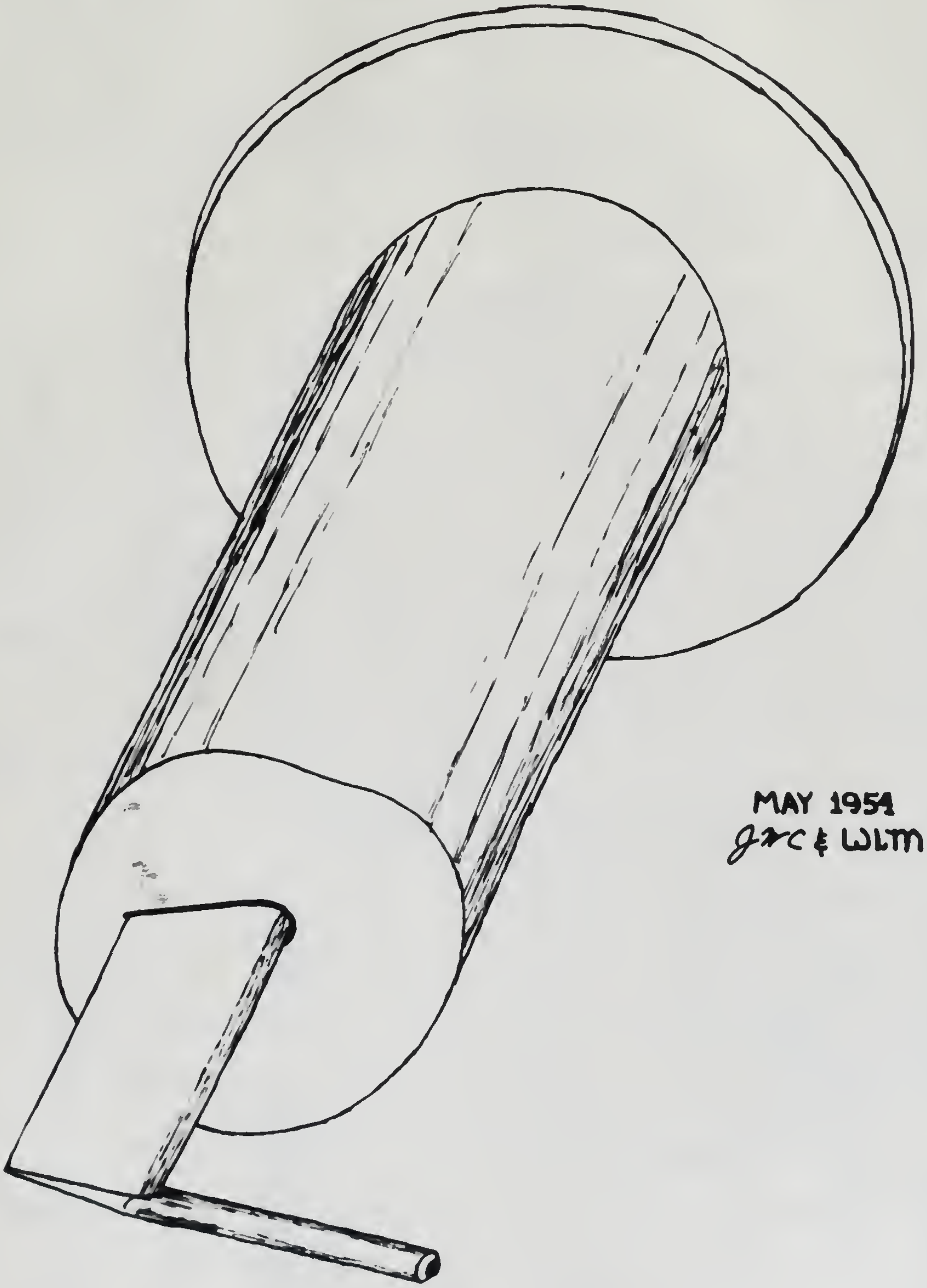

MAY 1954
JRC & WLM

SECTIONAL VIEW

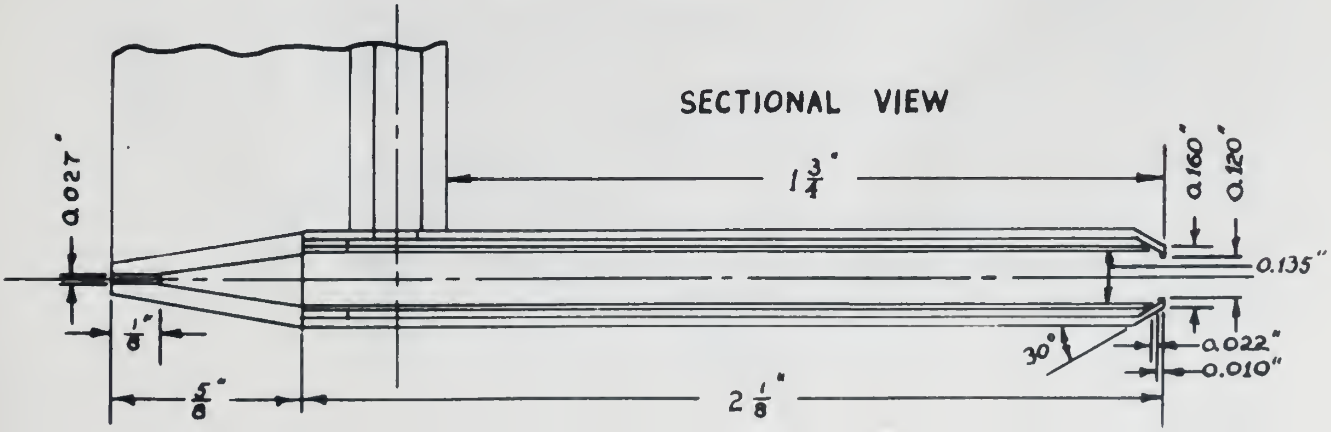

the water rate and static pressure differences at the plane of the probe tip were matched with those of his experiments.

C. Traversing Mechanism Construction

Preliminary investigation revealed that from a strictly mechanical viewpoint the most satisfactory traversing mechanism would be one that employed a manually operated, geared drive with a counter attached for accurately positioning the probes within the aerothermopressor; however, economic considerations point towards a more simply constructed mechanism. Such a simple device might consist of a mechanism merely to support the probe which could then be positioned by pushing in and pulling out the probe stem to which is attached a position indicating pointer.

Two designs based on the above criteria were developed and submitted for bids. The geared drive mechanism cost approximately $600 whereas the push-pull one cost $250; however, a fair economic evaluation must include a consideration of the overall cost of operating the large scale aerothermopressor with which the probes are to be used. For instance, since the fuel required to produce the hot gases for the aerothermopressor will cost approximately $35 per hour of operation, an appreciable saving in the time required for the taking of data assumes some economic significance. It is anticipated that the geared drive mechanism can be positioned accurately more rapidly and hence, may afford some

FIGURE II
SMALL SCALE TEST EQUIPMENT

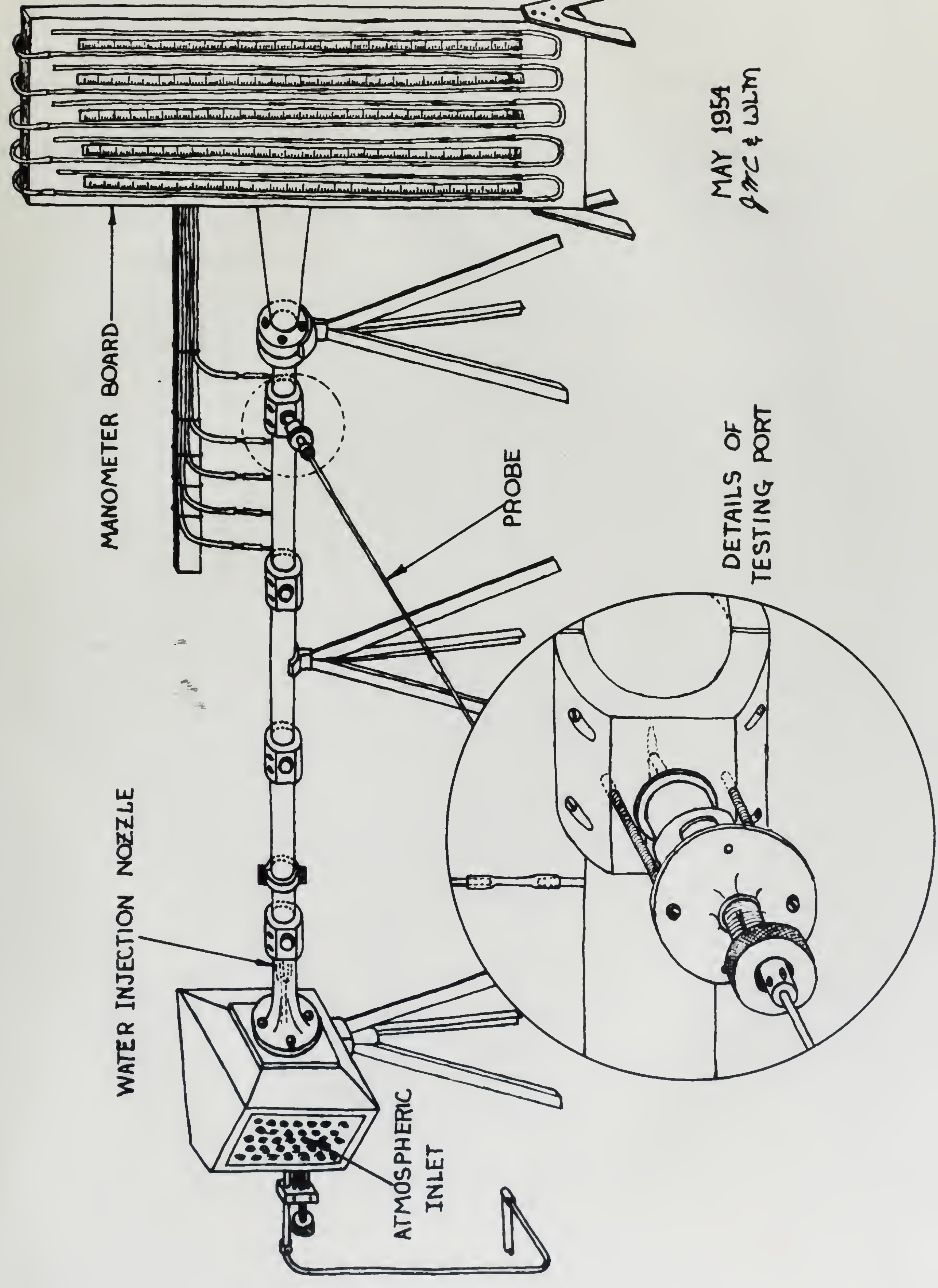

savings in operating time. In order to determine whether this saving would offset the increased initial cost, a mechanism of each type has been constructed for evaluation to guide future instrumentation design for the large scale aerothermopressor.

III. Results

Two probes were constructed, the heads of which are as shown in figure I. The stems of the two instruments differ in that one is threaded for use in the mechanically geared traversing mechanism, while the other is plain for use in the push-pull assembly. Two traversing mechanisms were constructed as illustrated in figure III.

The probes were tested in the small scale transparent equipment shown in figure II. The results of the tests are plotted in figures IV through X, along with the points determined by Dussourd in reference (3).

FIGURE III
PROBE TRAVERSING MECHANISM

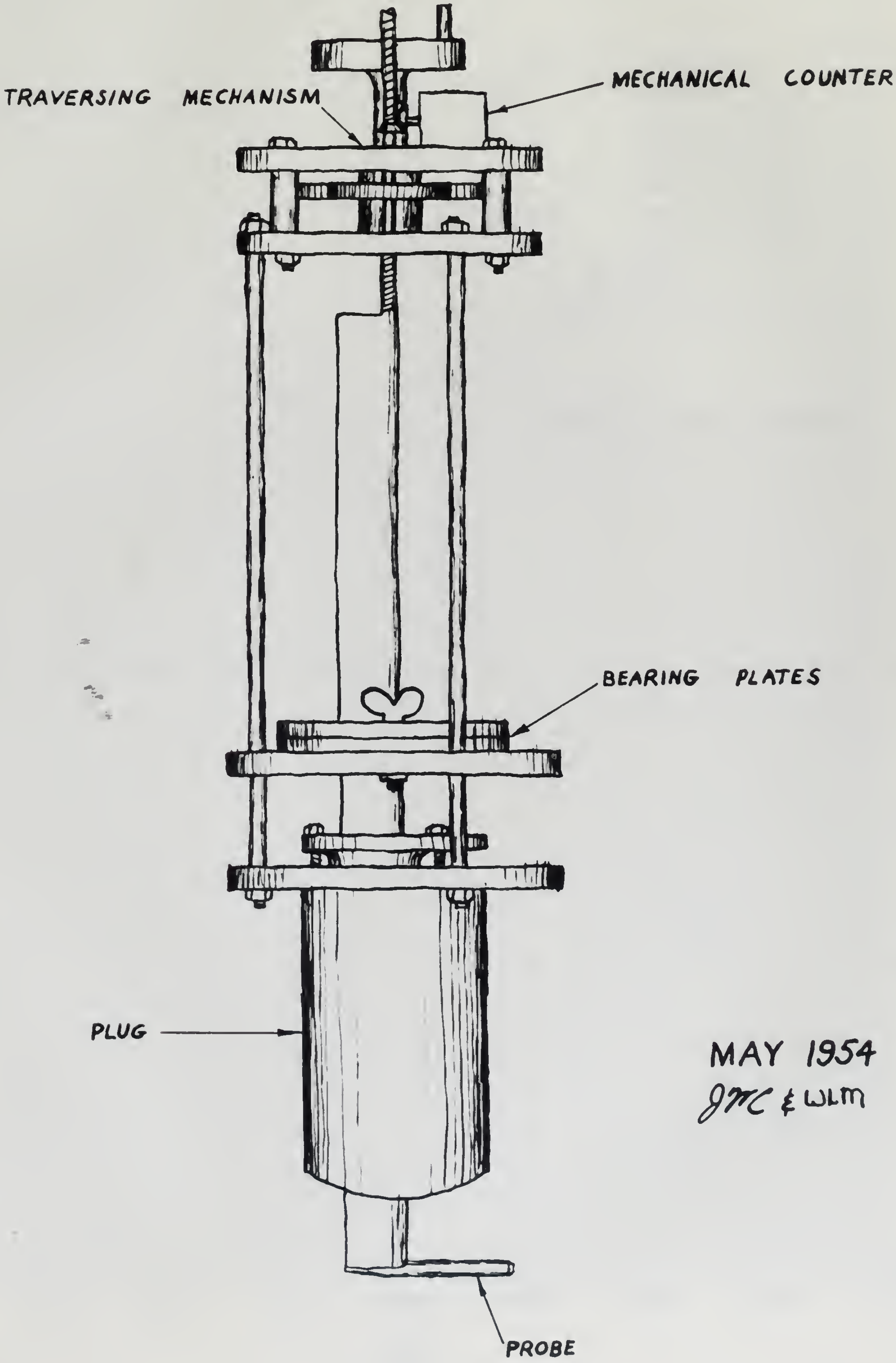

MAY 1954
JMC & WLM

FIGURE IV

NON-DIMENSIONALIZED, STAGNATION PRESSURE VS. STATIC PRESSURE

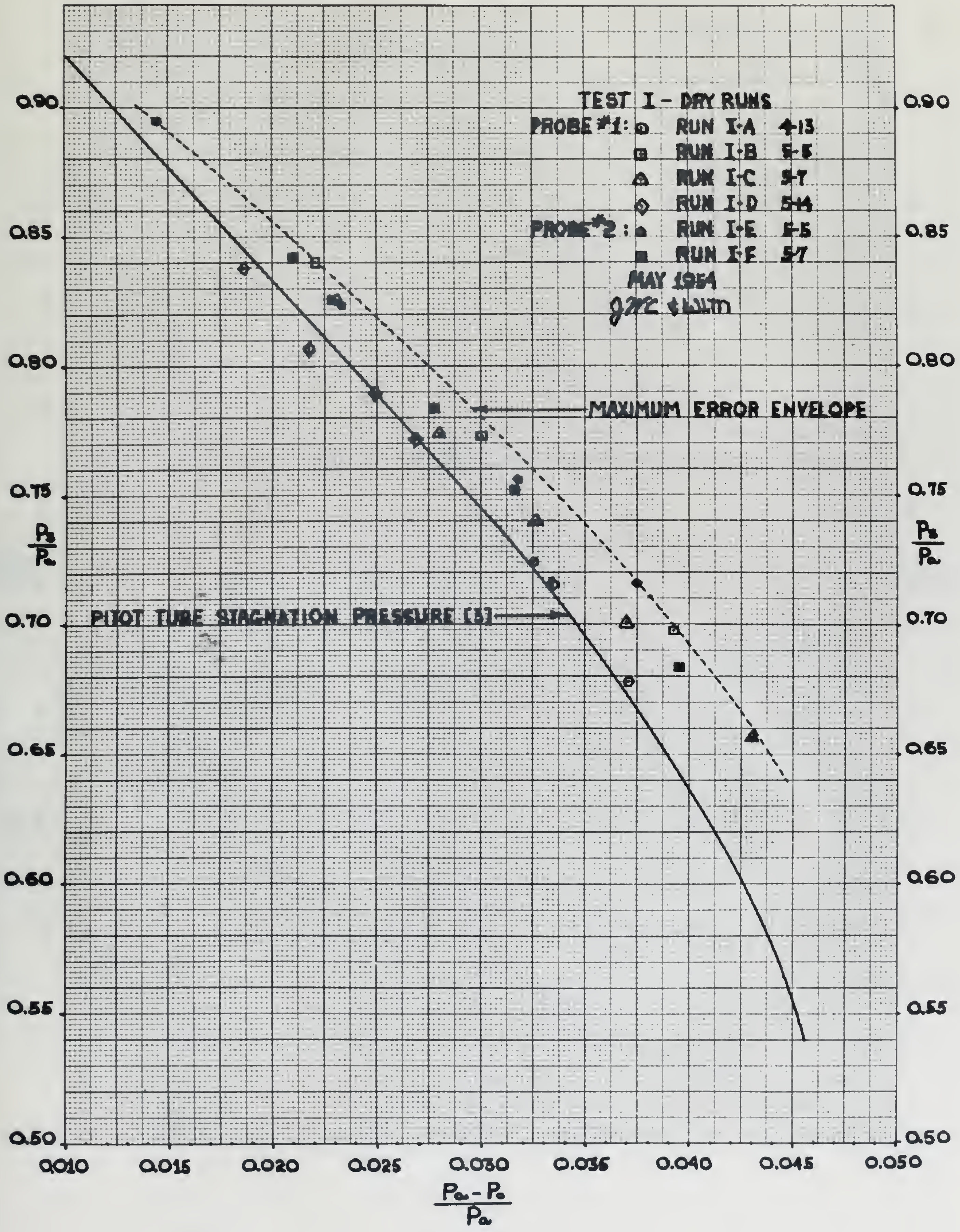

FIGURE V

NON-DIMENSIONALIZED, STAGNATION PRESSURE VS. STATIC PRESSURE

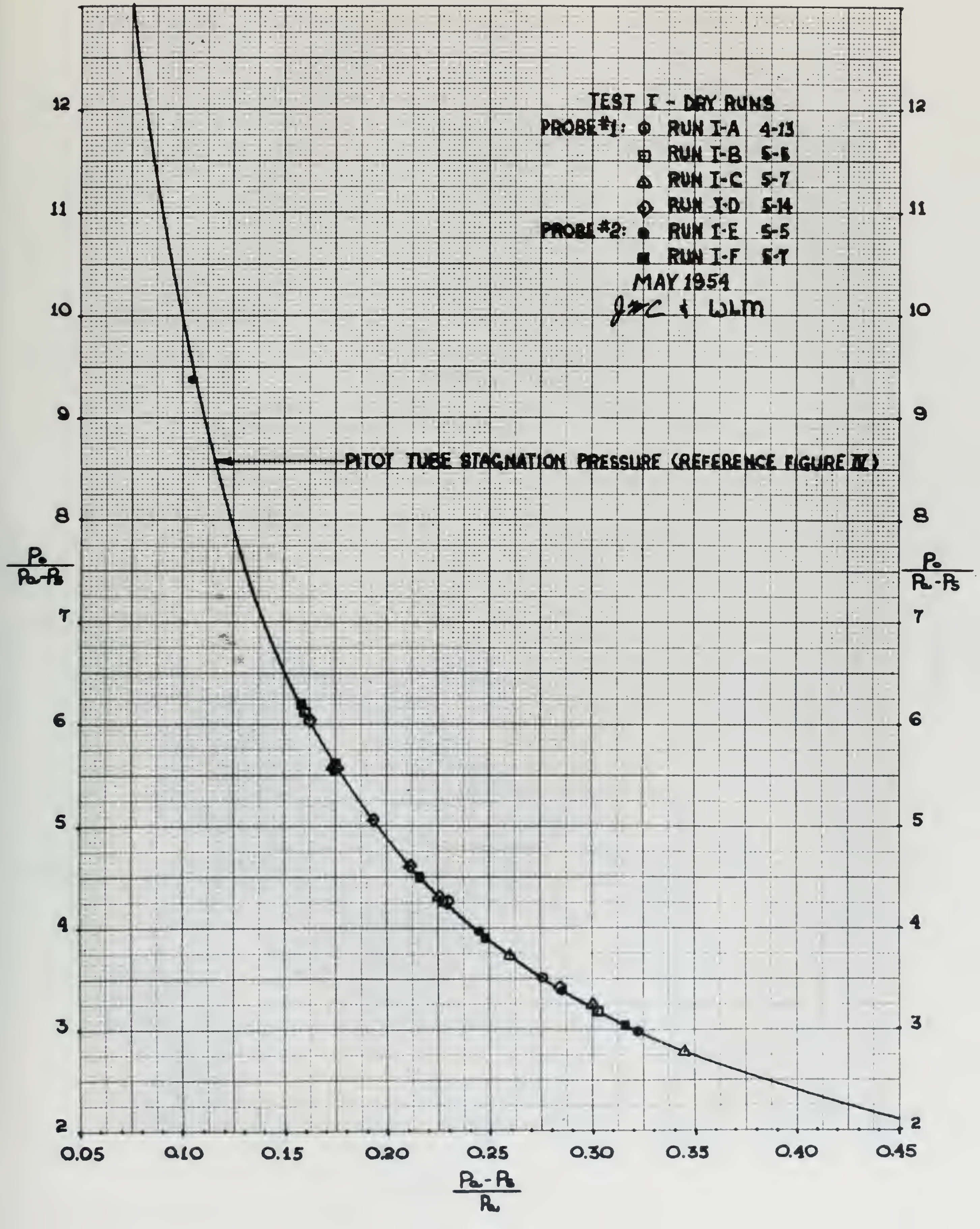

FIGURE VI
PROBE ERROR IN NORMAL AIR

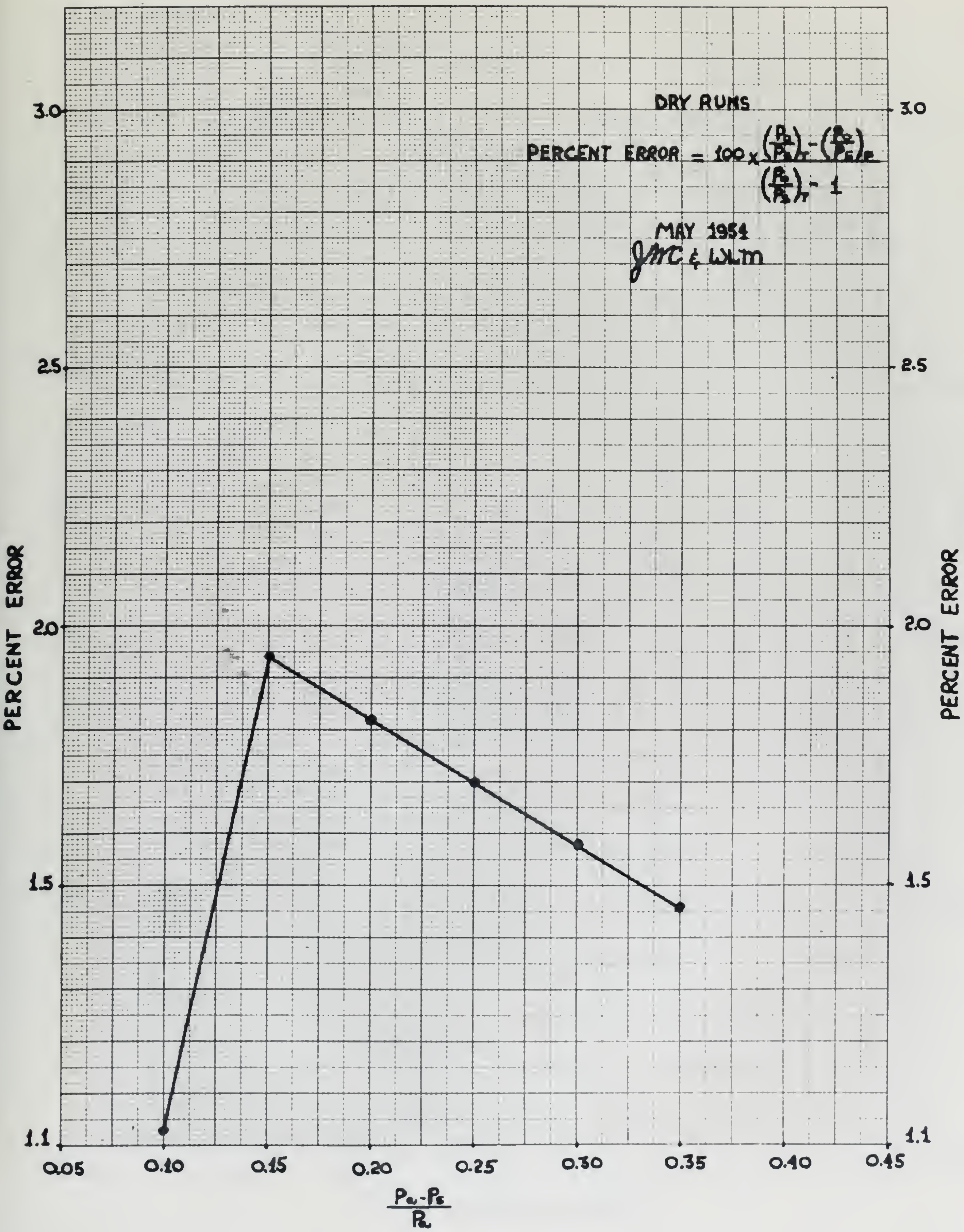

FIGURE VII

STAGNATION-STATIC PRESSURE RATIO — TEST II

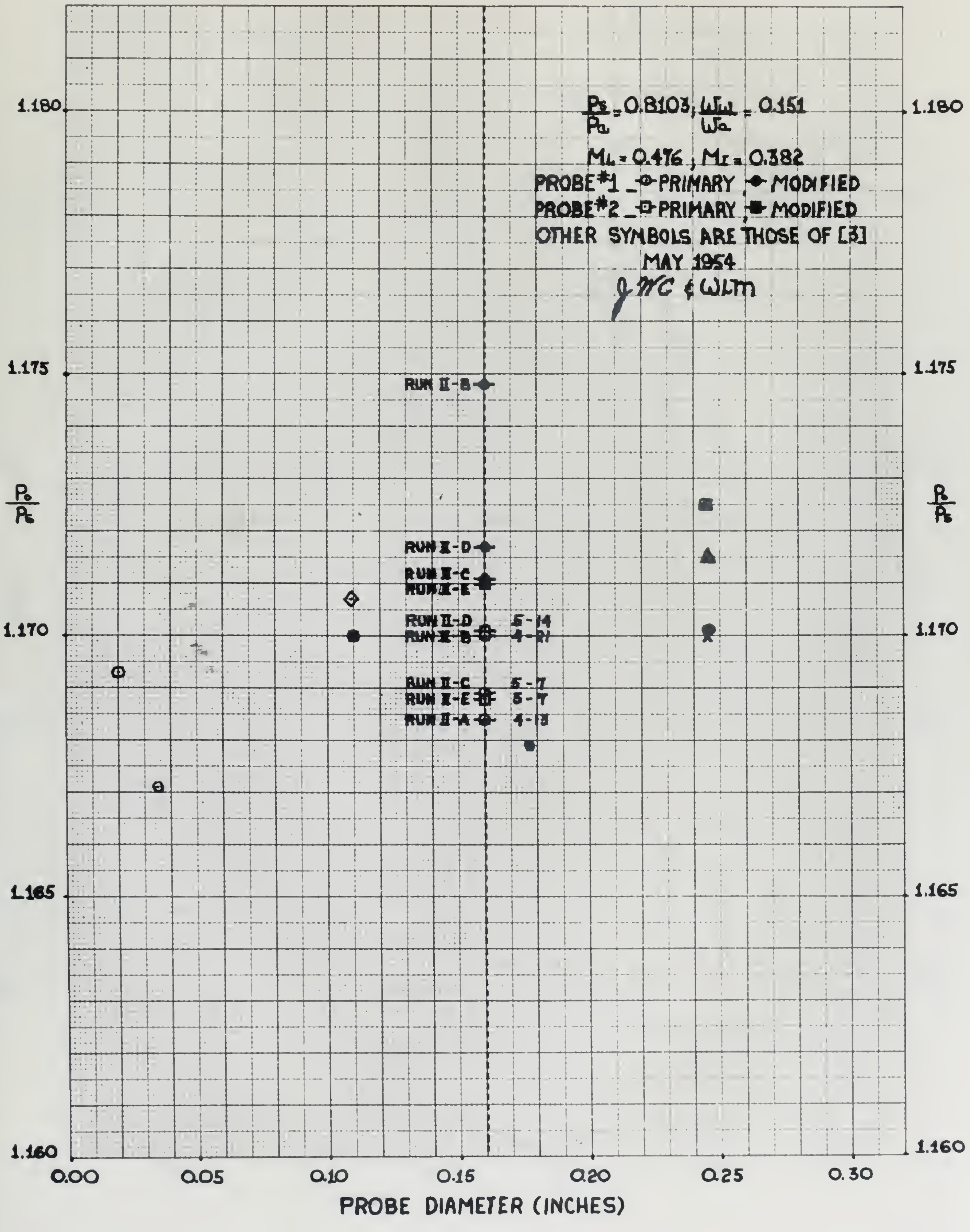

FIGURE VIII

STAGNATION-STATIC PRESSURE RATIO _ TEST III

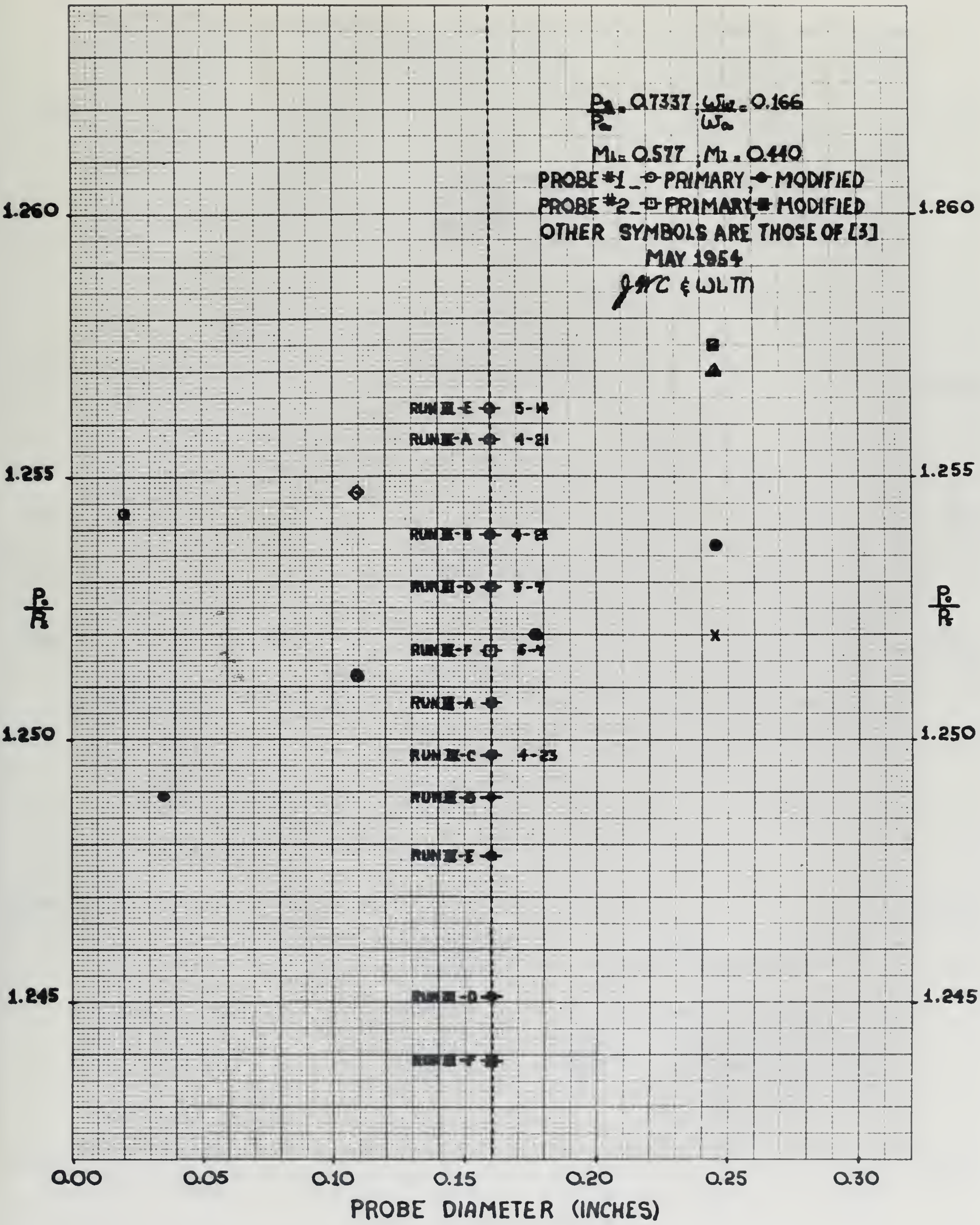

FIGURE IX

STAGNATION-STATIC PRESSURE RATIO — TEST IV

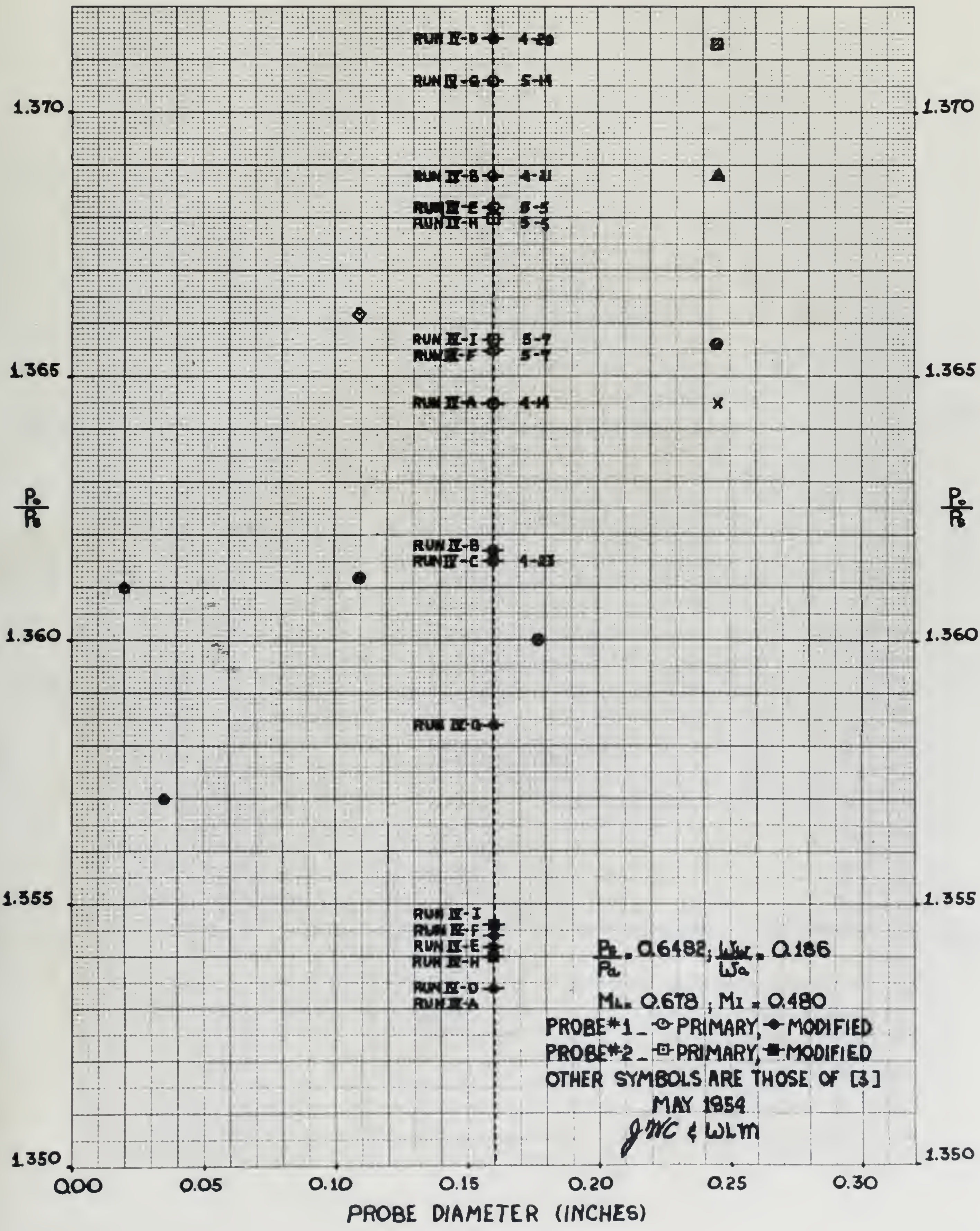

FIGURE X

STAGNATION-STATIC PRESSURE RATIO — TEST V

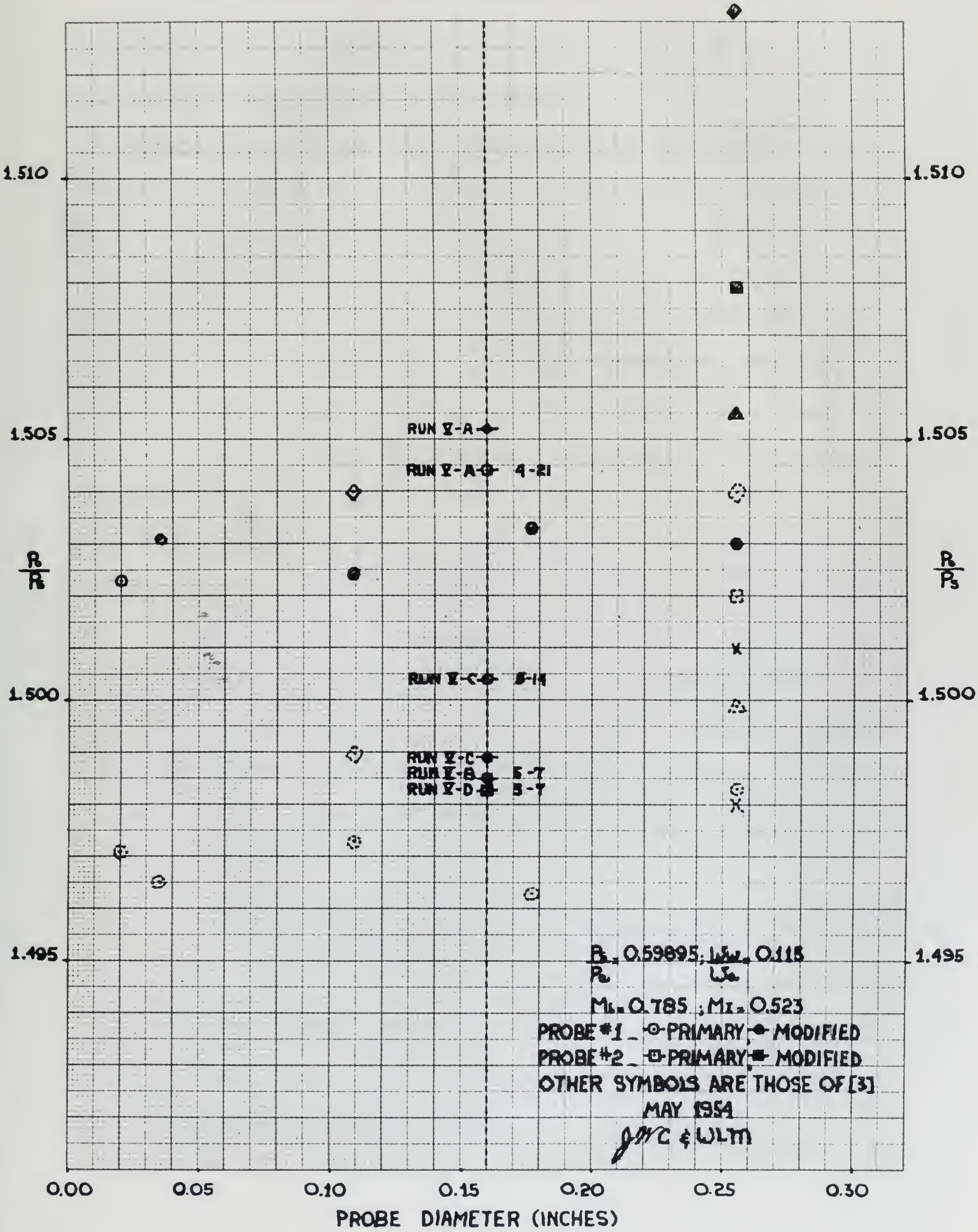

$\frac{P_1}{P_a}$ = 0.59895; $\frac{\omega_w}{\omega_a}$ = 0.115

M_1 = 0.785 ; M_2 = 0.523

PROBE #1 — ⊙ PRIMARY; ● MODIFIED

PROBE #2 — ⊡ PRIMARY; ■ MODIFIED

OTHER SYMBOLS ARE THOSE OF [3]

MAY 1954

JWC & WLM

IV. Discussion of Results

A. Probes' Measurements

Since these probes were constructed in accordance with criteria developed by Dussourd (3), the only data available on such a probe has been that obtained by his experiments. These probes were tested in the same equipment employed in the experiments of Dussourd. The authors, therefore, have attempted to correlate their data with his and match some of his operating points.

Dussourd calculated a non-dimensionalized curve of static pressure versus stagnation pressure for the dry air stream from measurements taken with a pitot tube. This curve is reproduced in figure IV. The curves representing these probes are superimposed on this plot (probe # 1 is that one constructed with a stem for the push-pull traversing mechanism, while probe # 2 is for use with the geared drive). The maximum percentage error in the measurements obtained by these probes is plotted on figure VI for the dotted envelope curve of figure IV. The error was computed as follows:

$$\text{percent error} = 100 \times \frac{(P_o/P_s)_{\text{pitot tube}} - (P_o/P_s)_{\text{probe}}}{(P_o/P_s)_{\text{pitot tube}} - 1}$$

The coordinates of figure IV were chosen in order to magnify the error of the probe; however, to give a more realistic presentation of the probes' performance the same data was replotted to the coordinates of figure V.

For wet flow conditions, the only data available for this type of probe is that of Dussourd(3); therefore, the performance of these probes for wet conditions could be evaluated by comparison of the measurements of these probes with those of Dussourd for identical flow conditions. The authors thought that identical flow conditions at the plane of the probe tip would be obtained if the water injection rate and the difference between atmospheric pressure and static pressure at the plane of the probe tip were matched with those of Dussourd. The primary data obtained in this manner and calculated as shown in appendix B-2 are plotted on figures VII through X, and are seen to correlate well with that of Dussourd.

By comparing the difference in the ratio of (P_o/P_s) for the maximum and minimum values and referring this difference to the minimum value as a base, the following percentage spread in the measurements of these probes was calculated:

$$\text{percent spread} = 100 \times \frac{(P_o/P_s)_{\text{max.}} - (P_o/P_s)_{\text{min.}}}{(P_o/P_s)_{\text{min.}} - 1}$$

The percentage spreads so determined for tests II through V are respectively, 1.01%, 2.64%, 2.74%, and 1.22%. These spreads were larger than was anticipated by the authors.

It was noted that these tests were conducted with water-air ratios that resulted in unsteady flow conditions, manifested by a fluctuating water wave in the diffuser which

resulted from normal boundary layer separation and the inclusion of water in the boundary layer. Such unsteadiness was not present in the experiments conducted by Dussourd as the reduction in flow area caused by his probes was less than the reduction caused by the probes of the authors. This unsteadiness caused violent fluctuation in the manometer levels which were damped out in order to obtain data. Consequently, instantaneous values for the observed data were not obtained but rather a time-average value was obtained. The value of this time-average depends upon the manner in which this unsteadiness occurs and for this reason, it was thought that this was a possible explanation for the spread.

For the days on which both probes were tested, it was noted that there was a negligible difference between their data points. From this it was concluded that there was no leakage or other fabrication errors in the construction of the probes.

The authors noted that for all four flow conditions the ratio (P_o/P_s) on April 21, was higher than that on May 7 (see primary data points of figure VII through X). Furthermore, for tests III and IV (see figures VIII and IX) the relative magnitudes of this ratio for April 21, May 7, and April 23 were the same (as noted on the figures not all tests were run on each day). This systematic variation suggested that the spread might be attributed to conditions that varied from day-to-day such as the pressure, temperature, and humidity of the atmosphere and the temperature of the injected water.

The temperature of the injected water was not measured and hence no analysis of this effect could be made. It was felt that the manner in which the data was correlated minimized the effects of atmospheric pressure variations. Since the maximum temperature variation of the air between all the test days was less than seven degrees Fahrenheit, it was felt that its effect could not account for the observed spread.

Analysis of the effect of the variation in atmospheric specific humidity revealed that the magnitude of the error introduced by neglecting this effect is of the same order of magnitude as that of the observed spread in the probe measurements. This analysis was carried out in the following manner:

The aerothermopressor process produces a rise in stagnation pressure by the lowering of the stagnation temperature of a high velocity gas stream. Conversely, it is also true that a stagnation pressure decrease will be obtained by raising the stagnation temperature of a high velocity gas stream. For the conditions in which these probes were tested, either process may occur depending on the specific humidity, initial mach number, initial air temperature, initial water temperature, etc. Complete analysis of this effect is beyond the scope of this thesis (see reference (2)).

The qualitative effect of the condensation of varying amounts of the humidity may be determined by making the following simplifying assumptions: (1) the difference in the amount of moisture which condenses for the various runs equals

the difference in specific humidities of the air for those runs; (2) all of this differential condensation occurs downstream of the nozzle. (Note that in the test apparatus, the plane of the water injection is downstream of the nozzle; hence, since the dewpoint temperature is reached as the air flows through the nozzle, the humidity of the air will condense and the injected water will not evaporate. It has been assumed in this analysis that the temperature of the injected water did not affect the air stagnation temperature); (3) the flow is one-dimensional; (4) the perfect gas relationships are valid; (5) atmospheric pressure is constant and; (6) there is isentropic flow through the nozzle.

For each test, the individual runs were modified by assuming that no condensation occured in that run, and then calculating the loss of stagnation pressure which would occur due to a rise in stagnation temperature if there were condensation equal to the difference between the specific humidity of each particular day and that of the day with the highest specific humidity.

The stagnation pressure was calculated by an iteration process using the influence coefficients of table 8.2 of reference (7), in which a single step was taken from the nozzle exit to the probe tip (actual iteration not carried out). The equation representing this process is as follows:

$$\frac{dP_0}{P_0} = -\frac{kM^2}{2}\left[\frac{dT_0}{T_0} + 4f\frac{dx}{D} + \frac{dX}{\frac{1}{2}kpAM^2} - 2y\frac{dw}{w} + 2\frac{dw}{w}\right]$$

integrating, $\ln \frac{P_{o2}}{P_{o1}} = -\frac{k\overline{M^2}}{2}\left[\ln \frac{T_{o2}}{T_{o1}} + \ln F\right]$

where subscripts (1) refers to the exit plane of the nozzle and subscripts (2) refers to the plane of the probe tip. Therefore, $\frac{P_{o2}}{P_{o1}} = \left(F \cdot \frac{T_{o2}}{T_{o1}}\right)^{-\frac{k\overline{M^2}}{2}}$

now letting the subscript (a) refer to the original condition and (b) refer to the condensing condition, and assuming: $F_a = F_b$; $\overline{M_a^2} = \overline{M_b^2}$; $(P_{o1})_a = (P_{o1})_b$.

and since the method of matching flow conditions implies that $(P_{s2})_a = (P_{s2})_b$, then

$$\frac{\left(\frac{P_{o2}}{P_{s2}}\right)_a}{\left(\frac{P_{o2}}{P_{s2}}\right)_b} = \frac{\left(\frac{T_{o2}}{T_{o1}}\right)_a^{-\frac{k\overline{M^2}}{2}}}{\left(\frac{T_{o2}}{T_{o1}}\right)_b^{-\frac{k\overline{M^2}}{2}}} = \left[\frac{(T_{o2})_a}{(T_{o2})_b}\right]^{-\frac{k\overline{M^2}}{2}}$$

$$\frac{\left(\frac{P_{o2}}{P_{s2}}\right)_a}{\left(\frac{P_{o2}}{P_{s2}}\right)_b} = \left[\frac{(T_{o2})_b}{(T_{o2})_a}\right]^{\frac{k\overline{M^2}}{2}} = \left[1 - \frac{\Delta T_{o2}}{(T_{o2})_a}\right]^{\frac{k\overline{M^2}}{2}}$$

By modifying the (P_o/P_s) ratios in the above manner, the modified data plotted on figures VII through X were obtained (see appendix B-3).

The difference between the primary and modified data points for a particular run is seen to be of the same order of magnitude as the observed spread of the primary data points. In view of the simplifying assumptions by which the modified data points were obtained, nothing other than the order of magnitude of the humidity effect can be inferred

from the modified data points.

As noted previously, the humidity effect is not the only source of error of these experiments. For instance, the humidity effect of tests II and V is in the opposite direction to some of the observed spread. It may well be that in these cases the effect of differences in injection water temperature among the various days was the governing factor.

These daily variation effects which may have caused the observed spread of the primary data points are important only insofar as they affect the calibration of these probes, and they will have negligible effect on the measurements obtained in the large scale aerothermopressor.

In view of the above analysis it is concluded that not all of the observed spread in the primary data points is due to inaccuracies in the probe measurements. However, even if all of the observed spread were due to the inaccuracy of the probes, the measurements obtained by the probes would still be valuable in the analysis of the large-scale aerothermopressor.

These probes have been designed to read the stagnation pressure in sub-sonic, droplet-laden, gas flows. If these probes are to be used in super-sonic, droplet-laden, gas flows, not only must the existance of the normal shock in front of the probe be taken into consideration when inter-

preting the pressure indicated by the probe, but also the severe deceleration of the water droplets which pass through the normal shock will have a strong effect on the pressure indicated by the probe, which effect must also be taken into consideration when interpreting the pressure indicated by the probe.

These probes have not been tested in supersonic flows.

D. Probe Strength

See appendix B-1 for the probe strength calculations.

As indicated in appendix B-1 these probes are not strong enough to withstand all types of flow conditions with the probe extended completely across an eleven inch duct.

Specifically, it is recommended that the use of the probes be limited in the following manner:

1. Do not extend the probes into a hot, dry gas flow any more than is necessary to obtain readings. Silver brazing has been used in the assembly of these probes and although the re-melt temperature of the silver alloy employed is 2000°F., this alloy will have little strength at high temperatures.
2. When the probe is extended into the duct during hot, dry runs, do not exceed a Mach number of 0.8. It is doubtful if the silver

brazing will be able to withstand the shear stresses imposed during hot, dry, trans-sonic flows.

3. During hot, dry runs never extend the probes more than 5.5 inches into the duct.
4. During wet runs when the Mach number is less than 0.8, the probe can be extended 11 inches into the duct.
5. During wet runs when the Mach number is greater than 0.8, the probe should not be extended more than 5.5 inches into the duct. If this limitation of extension of the probe is followed, the probe should be able to withstand all Mach number flows likely to be encountered.
6. During wet runs, if there is sub-sonic flow in the diffuser section the probe can be extended to the center line of the diffuser section.

C. Traversing Mechanism

The test and evaluation of the traversing mechanism must be carried out in the large-scale aerothermopressor, and therefore such tests must be conducted at a future date.

V. Conclusions

The probes as constructed will give satisfactory measurements of stagnation pressure in the large-scale aerothermopressor within the limits of expected experimental error.

The strength of these probes definitely is limited. It is felt, however, that if the limitations on the use of the probes as listed in the recommendations are followed, these probes will be able to be used without structural failure of any kind.

VI Recommendations

A. It is recommended that some consideration be given to the evaluation of the relative merits of the two traversing mechanisms from the viewpoints of economics and convenience.

B. Due to the limitation of the strength of the probes it is recommended that their use be restricted as follows:

1. Keep the probes out of the hot, dry gas flow as much as possible.
2. When the probe is used during hot, dry runs, do not exceed a Mach number of 0.8.
3. During hot, dry runs never extend the probe more than 5.5 inches into the duct.
4. During "wet" runs when the Mach number is less than 0.8, the probe can be extended 11 inches into the duct.
5. During "wet" runs when the Mach number is greater than 0.8, the probe should not be extended more than 5.5 inches into the duct.
6. During "wet" runs, if there is sub-sonic flow in the diffuser section, the probe can be extended to the center line of the diffuser section.

VII. Appendix

Appendix A-1

List of Symbols Used in Test

Symbols	
c	chord
C_D	drag coefficient
D	total drag force
F	$\epsilon\left[\int_1^2 4f\frac{dx}{D}+\int_1^2\frac{dx}{\frac{1}{2}kpAM^2}+\int_1^2(-2y+2)\frac{dw}{w}\right]$
I	moment of inertia
k	ratio of specific heats
l	length
M	Mach number
M	bending moment
P_a	atmospheric pressure
P_s	static pressure
P_o	stagnation pressure
R	gas constant
t	thickness
T_o	stagnation temperature
V	velocity
$\frac{w_w}{w_a}$	water-air ratio
$\Delta\frac{w_w}{w_a}$	difference in specific humidity
y	distance from neutral axis to fiber being considered
ρ	density
σ	stress

Nomenclature (cont.)

Symbols

μ	viscosity

Subscripts

$(\ )_a$	original condition
$(\ )_b$	condensing condition
$(\ )_I$	refers to initial condition
$(\ )_L$	refers to local conditions
$(\ )_p$	refers to probe
$(\ )_T$	refers to pitot tube
$(\ )_1$	exit plane of nozzle
$(\ )_2$	plane of probe tip

FIGURE XI

DIFFERENTIAL STATIC PRESSURE VS. DISTANCE ALONG TEST SECTION

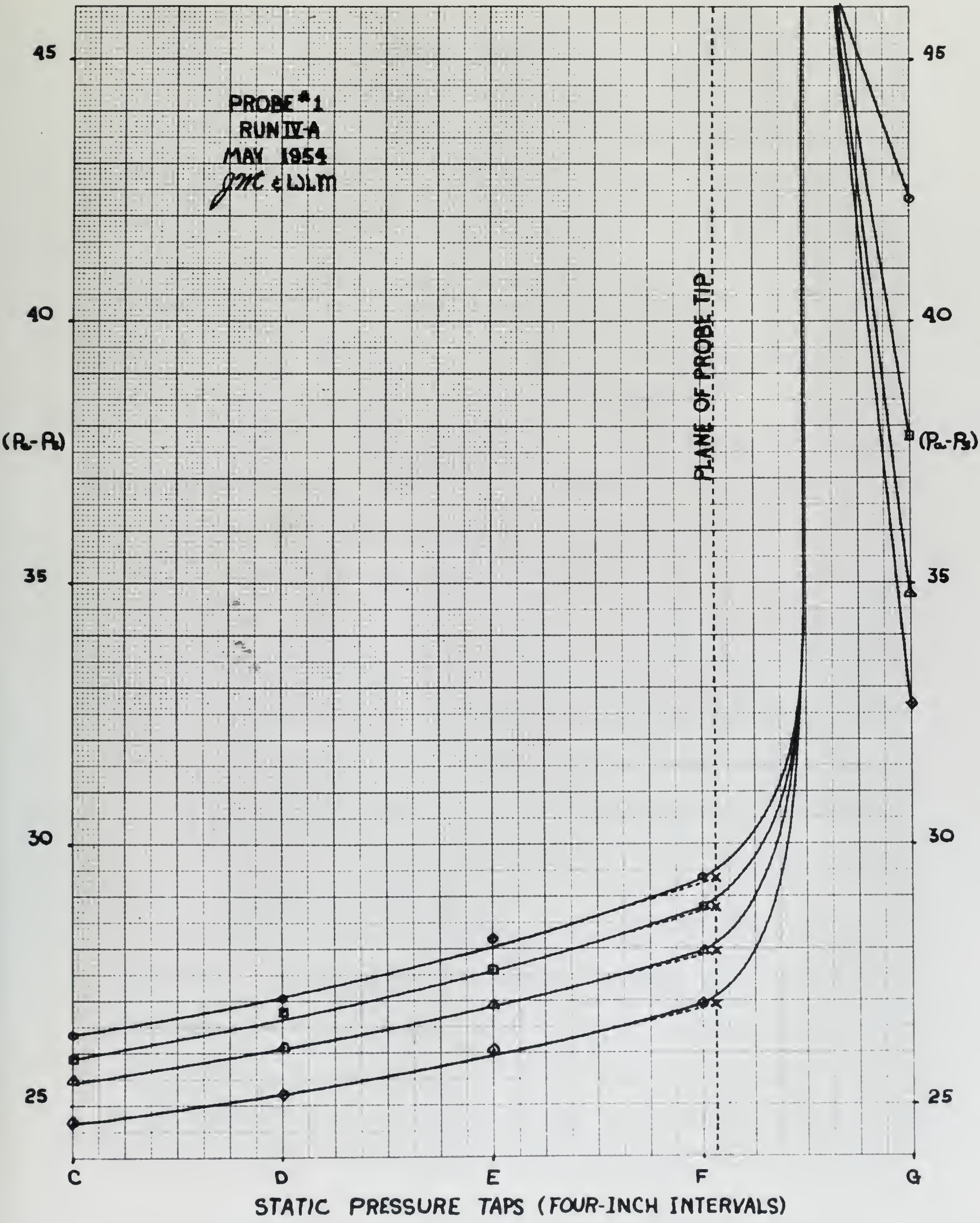

Appendix A-2

Details of procedure

Dussourd (3) presented his results as a plot of the ratio of the stagnation pressure to static pressure at the probe tip versus probe diameter for various ratios of static pressure at probe tip to atmospheric pressure (see figures V - VIII). In an attempt to match his operating points, the value of the ratio of the static pressure at the probe tip to atmospheric pressure was duplicated.

For several runs, a survey of static pressure versus distance along the test section was made to determine the correct value of static pressure at the probe tip - (see figure XI). It was found that extrapolation of the curve from the readings of pressure taps C, D, and E to the plane of the probe tip, in order to eliminate the effects of the pressure of the probe itself, resulted in a value of static pressure that was equal to that obtained from pressure tap F which is only slightly in front of the plane of the probe tip. Therefore, the reading of this pressure tap was used for all subsequent measurements.

For each wet run, a plot was made of $(P_a - P_s)$ versus $(P_a - P_o)$ - see figures XV - XVIII. The value of (P_s) corresponding to the correct ratio of (P_s/P_a) was then calculated and the corresponding value of $(P_a - P_s)$ was obtained. The aforementioned curves were then entered with this latter value of $(P_a - P_s)$ to determine the corresponding value of $(P_a - P_o)$.

With this value of stagnation pressure and the previously calculated static pressure, the ratio (P_o/P_s) was calculated and plotted on figures VII through X.

Appendix B-1

Probe Strength Calculations

The strength of these probes is limited, and therefore a certain amount of forethought must be employed in their use in order to avoid damaging the probes.

First, although the probes are made of type 304 stainless steel, silver brazing has been employed in the joining of the various parts of the probes: and in spite of the fact that the re-melt temperature of the silver alloy employed is 2000° Fahrenheit, it is recommended that the probes be exposed to high temperatures as little as possible, taking into consideration the value of using the probes to obtain measurements in a hot, dry gas flow.

Second, although these probes were designed primarily to measure the stagnation pressure in sub-sonic gas flows, it is recognized that these probes may be used in the trans-sonic and super-sonic regions of the aerothermopressor. In view of the fact that the shape of the probe-stem cross-section is a blunt nosed (i. e. subsonic) air foil shape, use of the probe in the trans-sonic and supersonic gas flows will result in high aerodynamic drag forces being imposed upon the probe. So that the orders of magnitude of these drag forces will be appreciated by the persons using these probes, the following strength calculations are presented.

The stresses occuring in the probe stem will be calculated

by simple beam theory assuming a uniform, cantilever type loading:

$$\sigma = \frac{My}{I}$$

where
D = total drag force
σ = stress (compressive or tensile)
$M = \frac{Dl}{2}$ = maximum bending moment
l = length of the equivalent cantilever beam
I = moment of inertia of the beam across-sectional area about its neutral axis.
y = the distance from the neutral axis to those fibers being considered. (usually the extreme fibers)

In order to compute the moment of inertia of the beam (probe-stem) cross-sectional area about its neutral axis, the stem cross-section will be simplified to a semi-circle at the base of a trapezoid with the hole in the probe stem centered at the junction of the semi-circle and trapezoid as shown:

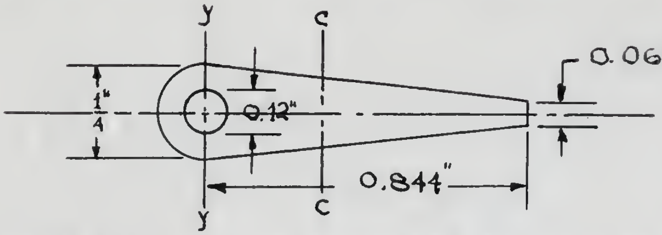

With this shape Iyy can be computed as follows:

$$I_{yy} = \frac{\pi(0.125)^4}{8} + \frac{(0.844)^3[3(0.0625) + 0.25]}{12} - \frac{\pi(0.06)^4}{4}$$

$$= 9.6 \times 10^{-5} + 2.19 \times 10^{-2} - 1.02 \times 10^{-5}$$

$$= 0.0218 \quad \text{in.}^4$$

The first moment about yy can be computed as follows:

$$M_{yy} = \frac{0.844}{3} \left(\frac{2(0.0625) + 0.25}{0.0625 + 0.25} \right) \frac{0.844(0.0625 + 0.25)}{2} - \frac{4(0.125)}{3\pi} \left(\frac{\pi(0.125)^2}{2} \right)$$

$$= 0.0445 - 0.0013$$

$$= 0.0432 \text{ in.}^3$$

The total cross-section area is as follows:

$$A = \frac{0.844(0.0625 + 0.25)}{2} + \frac{\pi(0.125)^2}{2} - \pi(0.06)^2$$

$$= 0.1320 + 0.0245 - 0.0113$$

$$= 0.1452 \text{ in.}^2$$

The center of area from yy is:

$$\overline{yy - cc} = \frac{M_{yy}}{A} = \frac{0.0432}{0.1452}$$

$$= 0.297 \text{ in.}$$

cc is the neutral axis.

Distance of cc from leading edge is:

$$y_1 = 0.297 + 0.125$$

$$= 0.422 \text{ in.}$$

Distance of cc from trailing edge is:

$$y_t = 0.844 - 0.297$$

$$= 0.547 \text{ in.}$$

The moment of inertia about the neutral axis, cc, is:

$$I_{cc} = I_{yz} - \overline{yy-cc}^{\,2} \; (A)$$

$$= 0.0218 - (0.297)^2 \; (0.1452)$$

$$= 0.0218 - 0.01282$$

$$I_{cc} = 0.00898 \text{ in.}^4$$

It is recognized that when there are water droplets in the gas stream, the drag force acting on the probe will be greater than for corresponding gas flows which contain no water droplets, due to the extra drag force caused by the momentum change of the water droplets which strike the probe. No attempt will be made here to compute the extra drag force caused by the water droplets. Instead, this analysis will assume isentropic flow of a perfect gas with constant specific heat and molecular weight with k = 1.4, for the purpose of computing the properties of the gas; and then experimentally determined drag coefficients will be employed to estimate the drag force. (The authors leave to the person using the probe the problem of estimating the effect that water droplets in the stream will have on the drag force, pointing out, however, that in addition to affecting the drag force directly, the water droplets will also change the flow conditions of the gas, for instance, by changing the temperature and density of the gas flow.)

The drag force will be computed by a formula of the type:

$$D = C_D \rho \frac{V^2}{2} (\text{area})$$

The density and velocity will be computed by isentropic processes as follows:

It is expected that the maximum stagnation temperature to be used in the aerothermopressor is 1500°F. or 1960° R. It is expected that the maximum pressure at the entrance to

the aerothermopressor will be 20 psig or 34.7 psia.

Therefore, considering the extreme case:

$$T_o = 1960^\circ \text{ R.}$$

$$P_o = 34.7 \text{ psia.}$$

$$\rho_o = \frac{P_o}{R\ T_o}$$

$$= \frac{34.7(144)}{53.35(1960(32.2))}$$

$$= 1.483 \text{ X } 10^{-3} \text{ slugs/ft.}^3$$

Let the subscript 2 designate the condition at the probe. Then:

$$\frac{T_2}{T_o} = f(M_2)$$

Reference (5) Table 30

$$\frac{\rho_2}{\rho_o} = f(M_2)$$

$$V_2 = 49 \sqrt{T_2}\ M_2$$

Now: C_D is to be determined from experimental data and the "area" must be chosen to fit the definition of C_D.

For the probe-stem cross-section:

t = thickness = 0.25 in.

c = chord = 1.00 in.

Therefore: $\frac{t}{c} = 0.25$

For subsonic compressible flow at low and moderate Mach numbers the compressibility effects of the flow have only a slight influence on the drag coefficient determined by incompressible flow measurements. When the local Mach number

at some point of the flow around the body exceeds unity, however, the drag coefficient begins to increase quite rapidly over the drag coefficient for incompressible flow. The free stream Mach number at which some local Mach number reaches unity is called the critical Mach number. The free stream Mach number at which the drag coefficient begins to increase rapidly is called the drag-divergence Mach number.

It is estimated that for Mach numbers higher than the drag-divergence Mach number the drag coefficient of the probe stem based on the frontal area will be almost the same as the drag coefficient of a circular cylinder in transversal flow based on the frontal area.

Figure 12.10 of reference (5) has a curve of C_D vs. M for a circular cylinder in transversal flow for trans-sonic flow. According to this curve the drag-divergence Mach number is 0.8, after which C_D rises to 2.13 for a Mach number of unity and falls again to 1.5 for a Mach number of 1.5.

Now, an estimate will be made of C_D for M = 0.8 for the probe stem. For the circular cylinder of reference (5), C_D = 1.5 at M = 0.8. This C_D will be compared to that for an airfoil shape at low Mach numbers.

$$M_2 = 0.8$$

$$\frac{T_2}{T_0} = 0.88652$$

$$\frac{\rho_2}{\rho_0} = 0.74000$$ Table 30 of Reference(6)

$$\rho_2 = 0.74000(1.483 \times 10^{-3})$$

$$= 1.099 \times 10^{-3}$$

$$T_2 = 0.88652\ (1960)$$

$$= 1738$$

$$V_2 = 49(0.8)\sqrt{1738}$$

$$= 1637 \text{ ft/sec}$$

$$\text{Reynolds Number} = \frac{\rho_2 V_2 c}{\mu_2}$$

$$\mu_2 = \frac{278}{32.2} \times 10^{-7}$$ Table 2 Reference (6)

$$= 8.63 \times 10^{-7} \text{ slugs/sec. ft.}$$

$$\text{Reynolds number} = \frac{(1.099 \times 10^{-3})(1637)}{(12)(8.63 \times 10^{-7})}$$

$$= 1.735 \times 10^{5}$$

According to figure 5.1 of reference (5):

For Reynolds Number = 1.735×10^{5} and t/c 0.25

$C_D = 0.06$ based on the wetted area.

The wetted area is about eight times the frontal area for the probe stem; and therefore, when the C_D is based on the frontal area it will be : $C_D = 0.48$

The ratio of these drag coefficients at M = 0.8 is

$$\frac{C_D \text{ cyl.}}{C_D \text{ airfoil}} = \frac{1.5}{0.48} = 3.12$$

It can be stated that the C_D for the probe stem will be larger than 0.48 both because of compressibility and because the maximum thickness of the probe stem occurs at 12.5% of the chord. It can also be stated that C_D will be less than 1.5 since the probe-stem is a more "streamlined" shape than a cylinder.

In order to be conservative in this analysis the authors assume that for M = 0.8 the C_D for the probe stem is 1.5 based on the frontal area.

The drag force and maximum stress will be computed for the following assumed conditions:

M_2	0.8	0.9	1.0	1.1	1.2	1.5
C_D	1.5	2.13	2.13	2.13	2.13	1.5

For convenience it will be assumed that the probe tip has the same drag force as 1/8 inch of stem. Therefore when the probe is in the center of the test section ℓ = 5.5 inches. The drag force and maximum stress will be computed for ℓ = 5.5 inches. The drag force will vary directly as ℓ and the maximum stress will vary directly as ℓ^2.

For ℓ = 5.5 inches

$$\text{Frontal area} = \frac{5.5(0.25)}{144} = 0.00955 \text{ sq. ft.}$$

FIGURE XII
DRAG COEFFICIENT VS MACH NUMBER

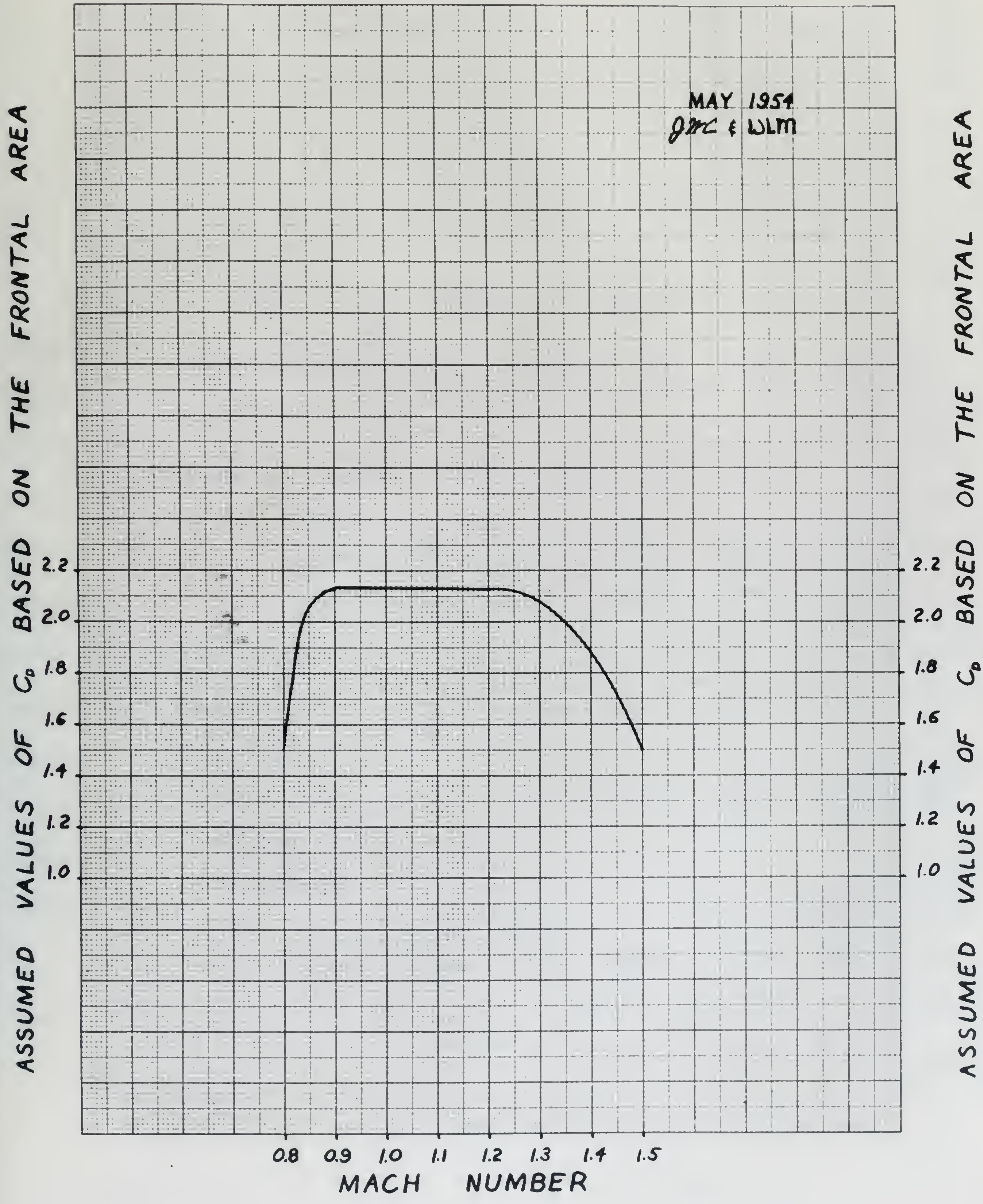

MAY 1954
JMC & WLM

Table I

Summary of Maximum Stress Calculations

M_2	0.8	0.9	1.0	1.1	1.2	1.5	
C_D	1.5	2.13	2.13	2.13	2.13	1.5	
ρ_0	1.483×10^{-3}						
$\frac{\rho_2}{\rho_0}$	0.74000	0.68704	0.63394	0.58169	0.53114	0.39498	
ρ_2	1.090×10^{-3}	1.020×10^{-3}	9.40×10^{-4}	8.63×10^{-4}	7.88×10^{-4}	5.86×10^{-4}	slugs/ft.^{3}
T_0	1960° R.						
$\frac{T_2}{T_0}$	0.88652	0.86058	0.83333	0.80515	0.77640	0.68965	
T_2	1738	1688	1633	1580	1522	1350	° R.
V_2	1637	1815	1980	2142	2297	2702	ft/sec.
Area =	0.00955 ft.^{2}						
D	21.05	34.2	37.5	40.4	42.3	30.8	lbs.
ℓ	5.5 inches						
M	57.8	94.0	103.1	111.1	116.3	84.7	lb-in $\frac{D\ell}{2}$
y	0.547 in.						
I	0.00898 in.^{4}						
σ	3520	5730	6280	6770	7080	5160	psi $\ell = 5.5$ in
σ	14080	22920	25120	27080	28320	20640	$\ell = 11$

(Note: although these stresses were computed for the case in which $T_0 = 1960^0 R$; for constant Mach number, constant P_0, and perfect gas relationships, the product $\rho_2 V_2^2$ does not vary with T_0 and therefore if these stresses are plotted against Mach number they will be valid for all values of T_0.)

FIGURE XIII
MAXIMUM STRESS VS MACH NUMBER

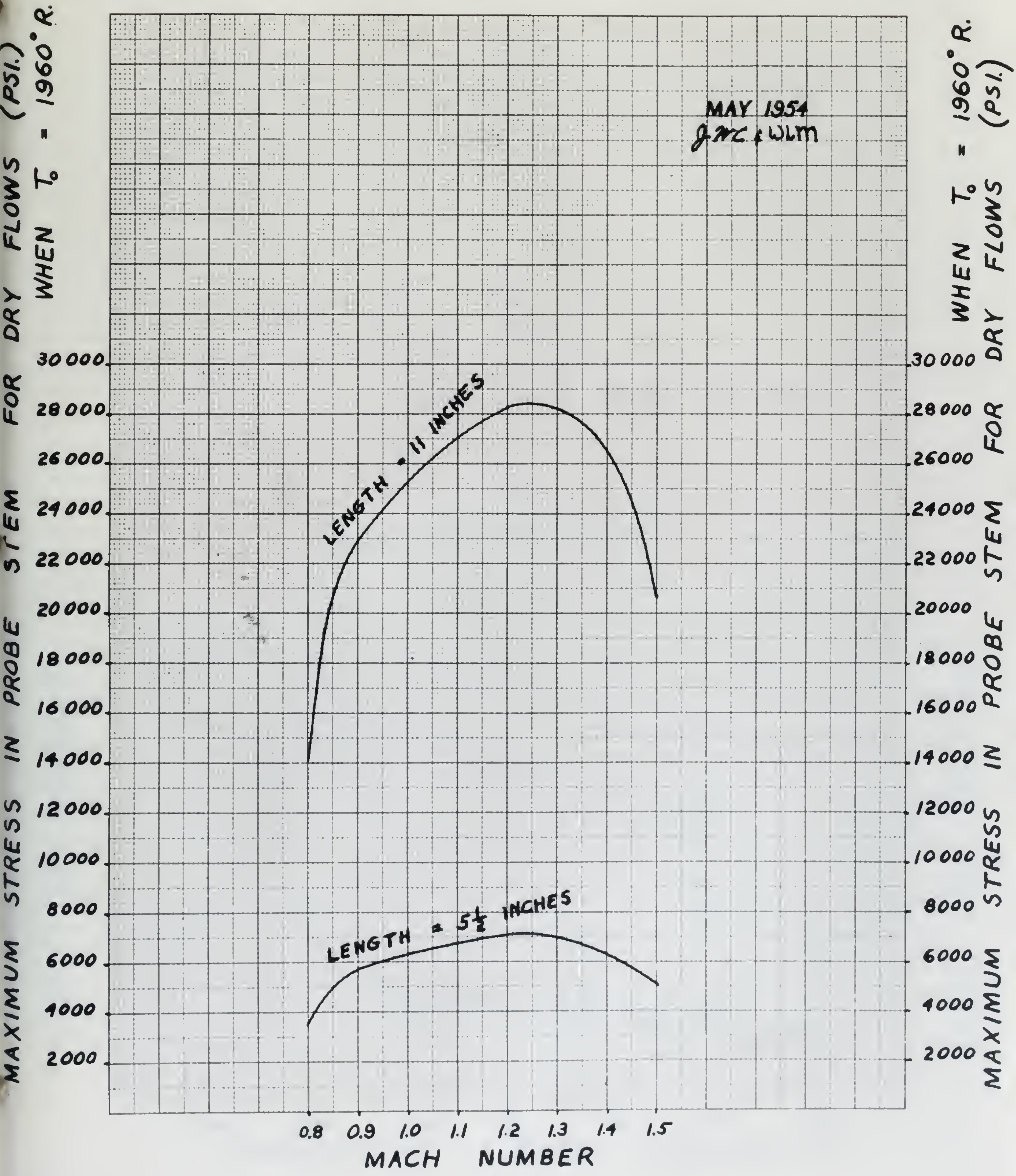

MAY 1954
JWC & WLM

FIGURE XIV

STRENGTH PROPERTIES OF STAINLESS STEEL TYPE 304

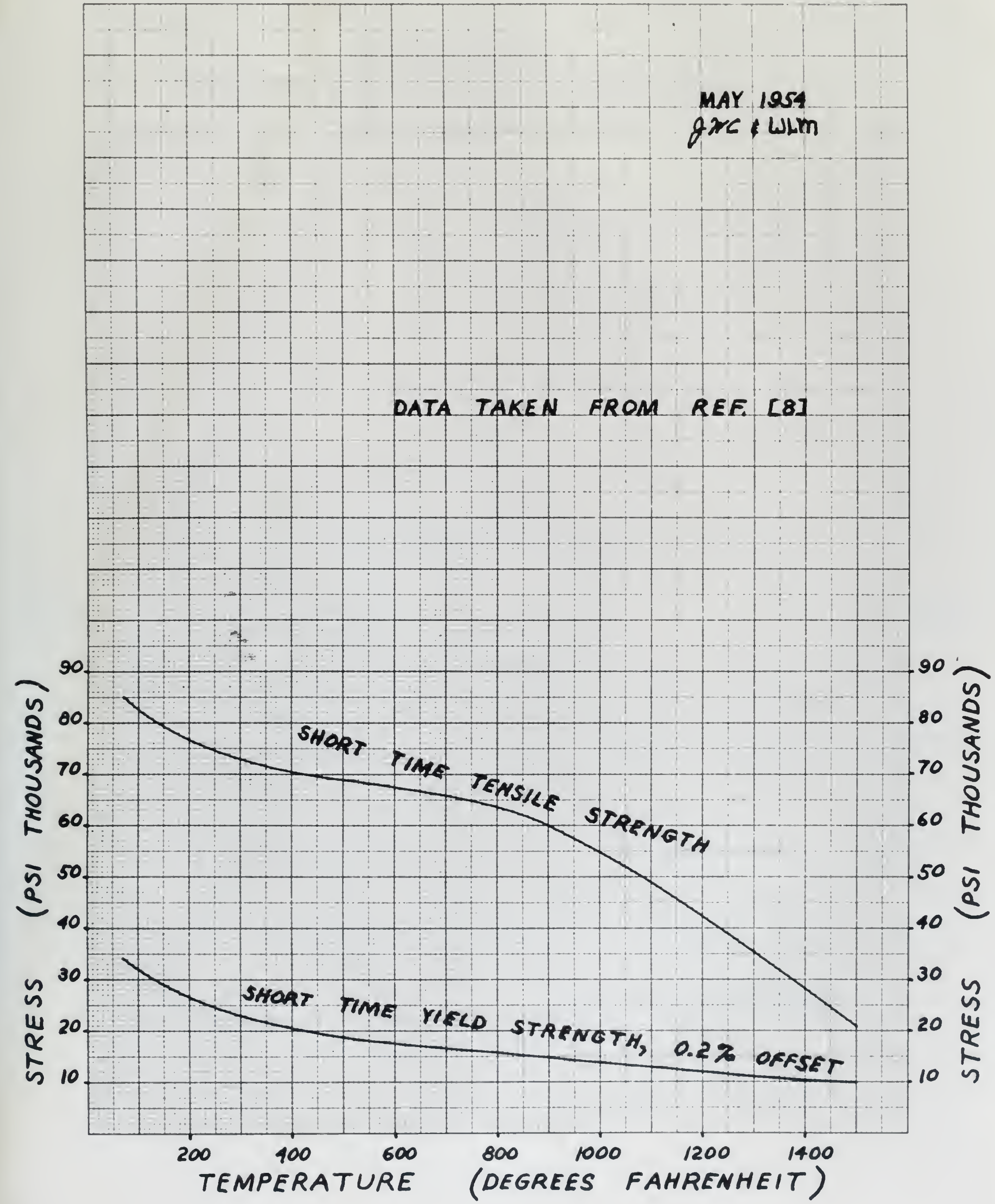

MAY 1954
JWC & WLM

DATA TAKEN FROM REF. [8]

Appendix B-2

Sample of Primary Data Point Calculations

Test II - 0.100 lbs/sec water

Probe #1 - Run II-A 4/13/54

p_A = 30.024 inches Hg. X 2.54 cm/inch = 76.261 cm. Hg.

$$(p_A - p_0) = 49.29 \text{ cm. } H_2O \times \frac{1 \ (\text{s.g. } H_2O)}{13.55 \ (\text{s.g. Hg})} = 3.638 \text{ cm. Hg.}$$

$(p_A - p_0)$ cm. Hg.	$(p_A - p_S)$ cm. Hg.
3.638	12.52
4.035	14.37
4.310	16.02

A curve of the above values is plotted on figure XV.

p_S/p_A = 0.8103

p_S = (0.8103)(76.261) = 61.794 cm. Hg.

$p_A - p_S$ = 76.261 - 61.794 = 14.467 cm. Hg.

Now referring to the above plot on figure XV, the value of $(p_A - p_0)$ corresponding to the above value of $(p_A - p_S)$ is found to be-

$(p_A - p_0)$ = 4.062 cm. Hg.

p_0 = 76.261 - 4.062 = 72.199 cm. Hg.

Therefore, $\frac{p_0}{p_S} = \frac{72.199}{61.794} = 1.1684$

This value is then plotted on figure VII of the results.

Appendix B-3

Sample of Modified Data Point Calculations

Test II - 0.100 lbs/sec, injected water

Probe #1 - Run II-B - 4/21/54

$M_I = 0.382 \qquad M_I^2 = 0.1459$

$M_L = 0.476 \qquad M_L^2 = 0.2266$

$$\overline{M^2} = \frac{M_I^2 + M_L^2}{2} = \frac{0.3725}{2} = 0.1862$$

$$\frac{k\overline{M^2}}{2} = \frac{(1.4)(0.1862)}{(2)} = 0.13034$$

specific humidity = 0.0083 lbs water/lb air

reference specific humidity (4/13/54) = 0.0045 lbs water/lb air

$\Delta\,(w_w/w_a) = 0.0045 - 0.0083 = -0.0038$ lbs water/lb air

$$w_w \, \Delta \, hfg = w_a C_p \, \Delta T_{02}$$

$$\Delta T_{02} = w_w/w_a \, \frac{\Delta hfg}{C_p} = (-0.0038)\left(\frac{1054.3}{0.24}\right) = (-0.0038)(4393)$$

Therefore, $\Delta T_{02} = -16.68$

$$(1 - \Delta T_{02}/T_{02_a})^{k\overline{M}^2/2} = [1 - (-16.68)/530\,]^{0.13034} = (1 + 0.03147)^{0.1303}$$

$$= (1.03147)^{0.13034} = 1.00410$$

$$(P_0/P_S)_{Mod.} = (P_0/P_S)_{Orig.}(1.00410) = 1.1700(1.00410) = 1.1748$$

This value is then plotted on figure VII of the results.

FIGURE XV

DIFFERENTIAL STATIC PRESSURE VS. DIFFERENTIAL STAGNATION PRESSURE

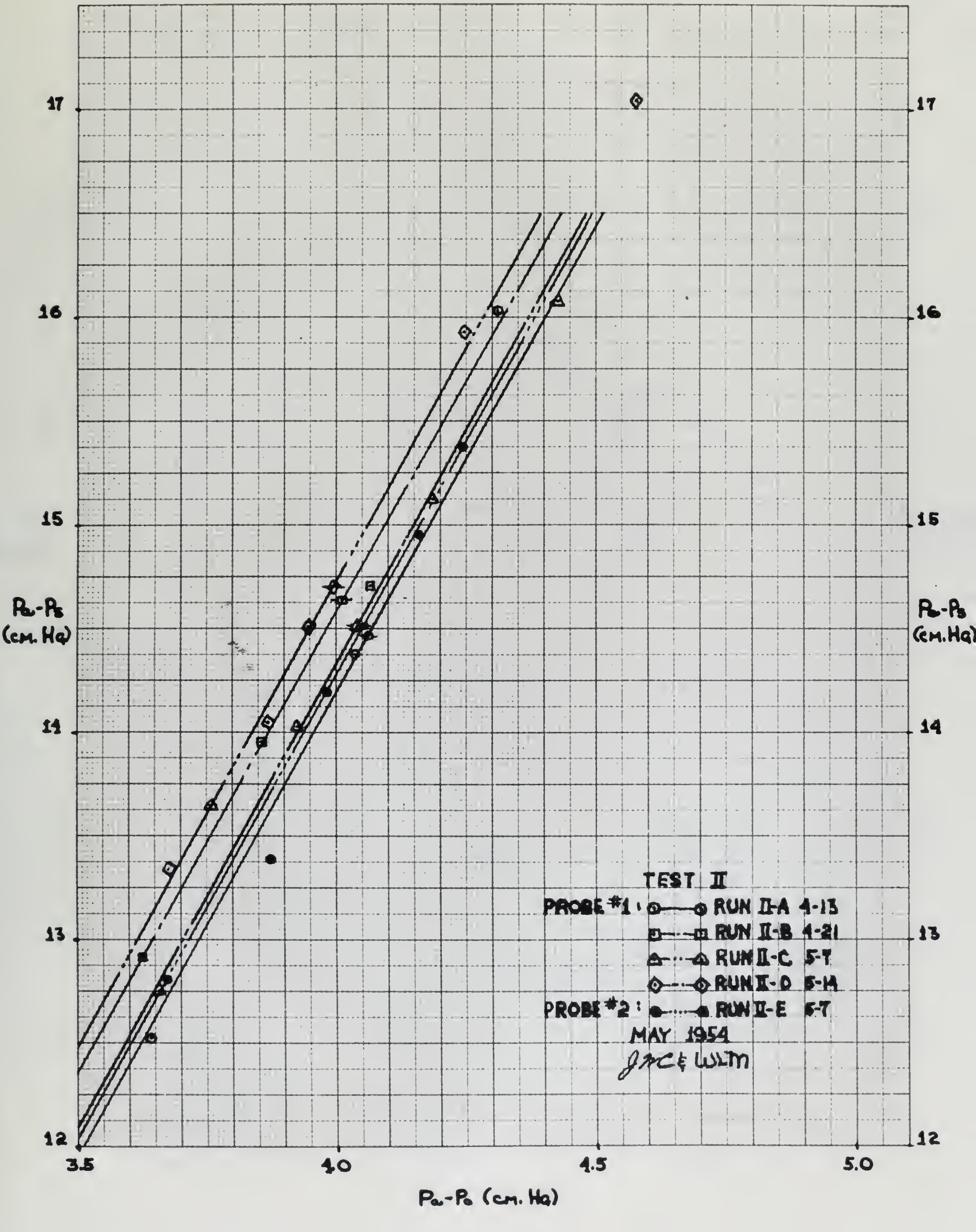

FIGURE XVI

DIFFERENTIAL STATIC PRESSURE VS DIFFERENTIAL STAGNATION PRESSURE

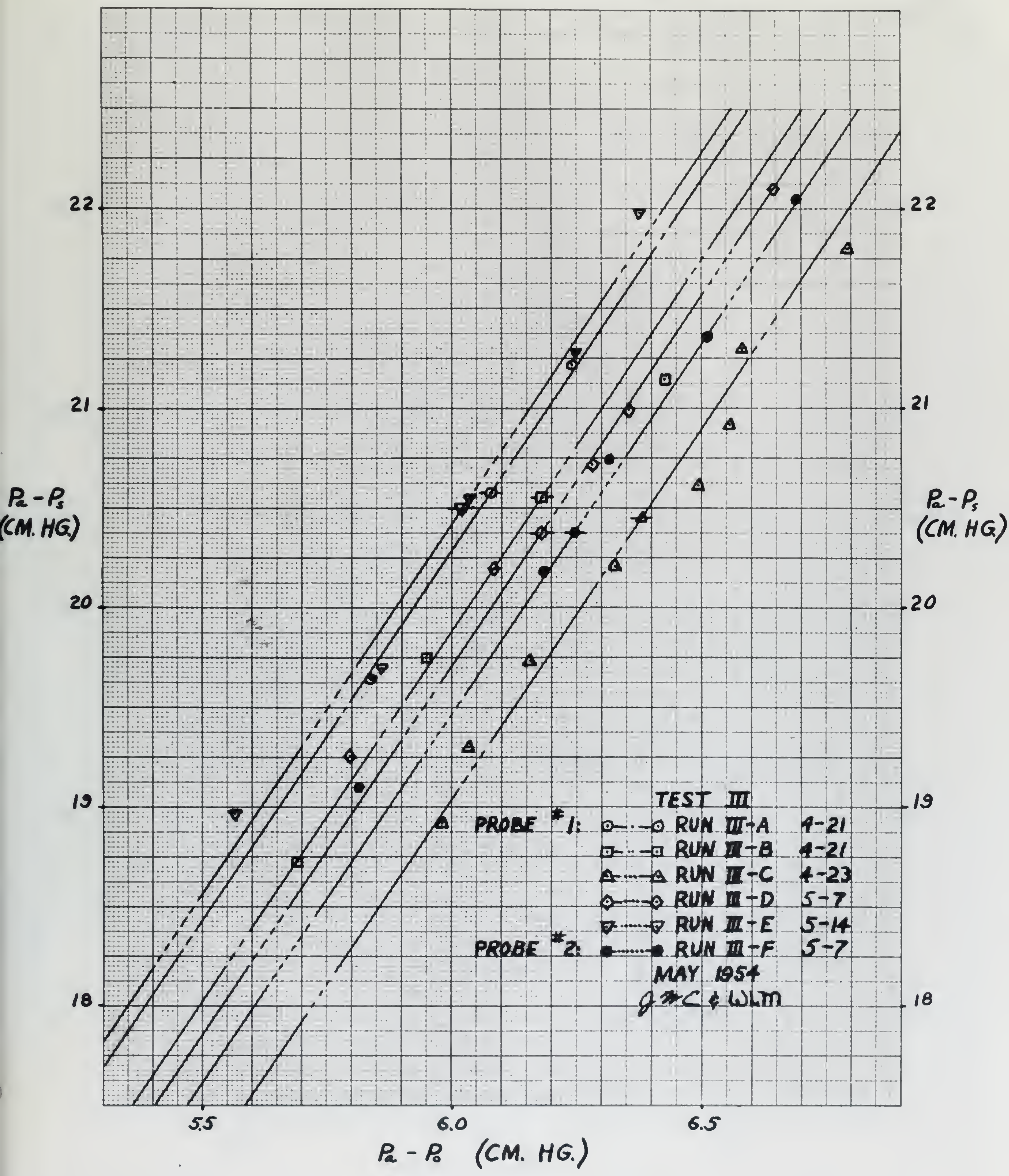

FIGURE XVII

DIFFERENTIAL STATIC PRESSURE VS. DIFFERENTIAL STAGNATION PRESSURE

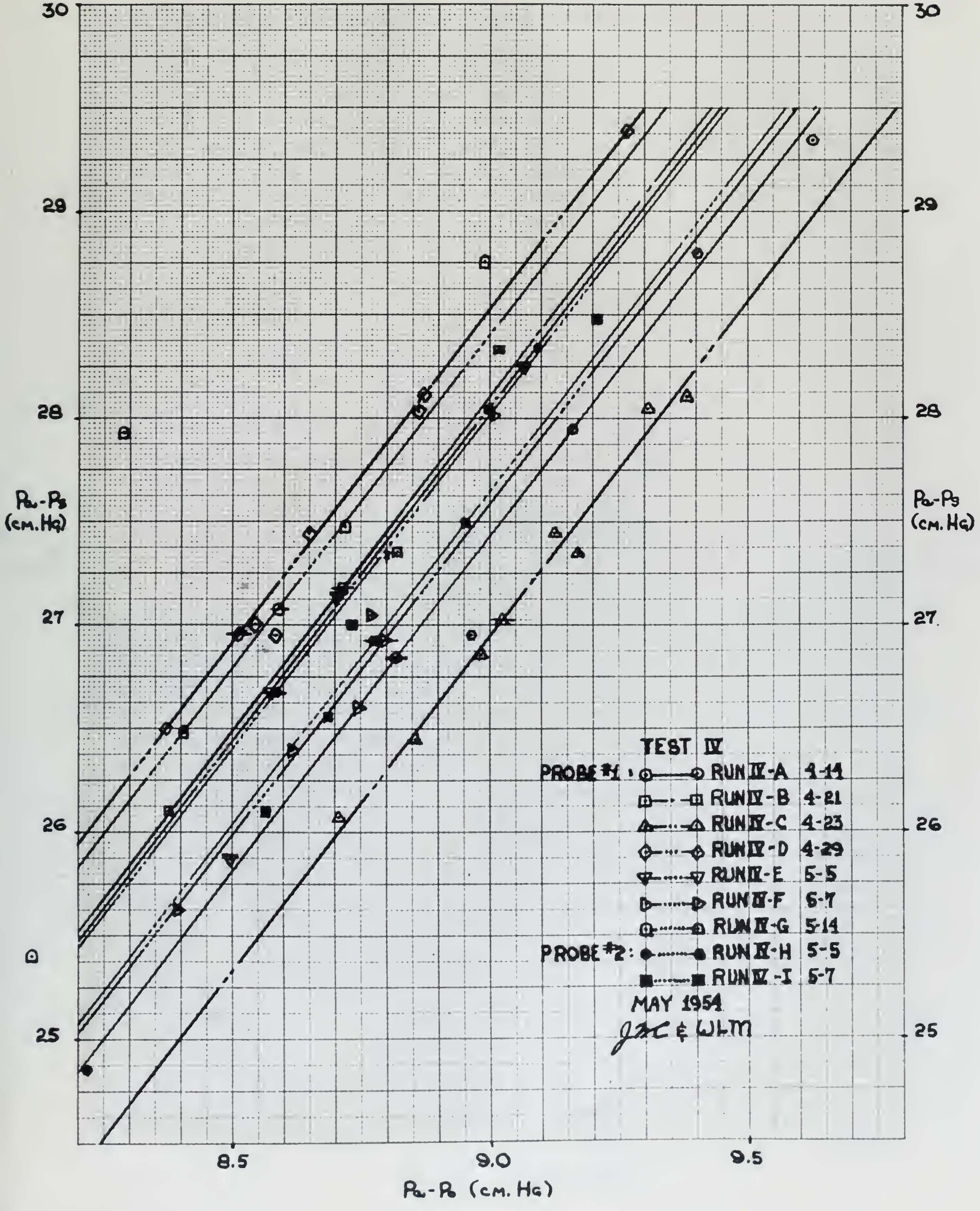

FIGURE XVIII

DIFFERENTIAL STATIC PRESSURE VS DIFFERENTIAL STAGNATION PRESSURE

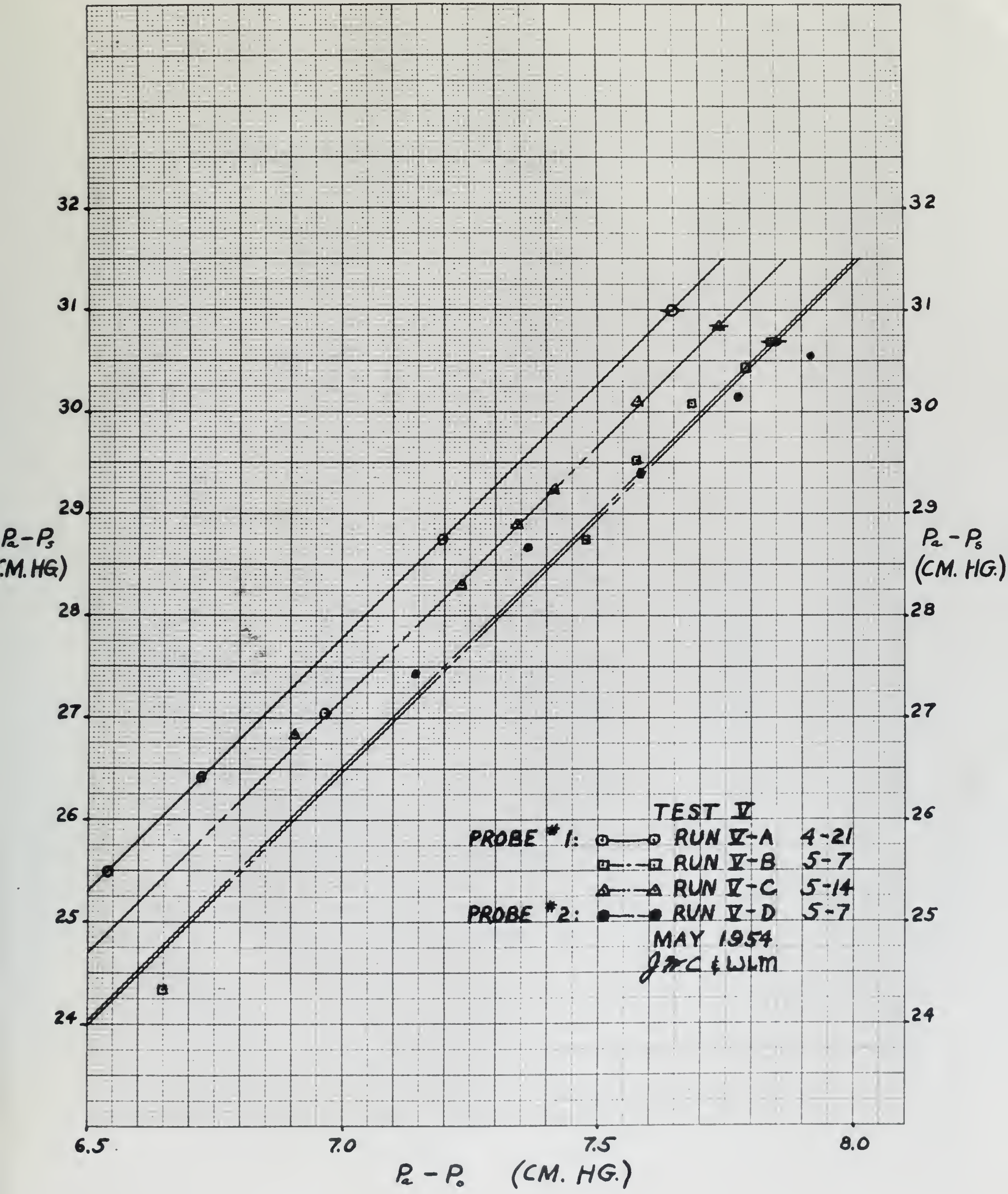

Appendix C-1

Table II

Summary of Dry Run Calculations (Pitot Tube)

(P_s/P_a)	$(P_a-P_s)/P_a$	$(P_a-P_o)/P_a$	(P_o/P_a)	(P_o/P_s)
0.920	0.080	0.010	0.990	1.076
0.878	0.122	0.015	0.985	1.122
0.834	0.166	0.020	0.980	1.175
0.789	0.211	0.025	0.975	1.236
0.745	0.255	0.030	0.970	1.302
0.693	0.307	0.035	0.965	1.392
0.637	0.363	0.040	0.960	1.507
0.556	0.444	0.045	0.955	1.718

(P_a/P_o)	(P_s/P_o)	$(P_a-P_s)/P_o$	$(P_o)/(P_a-P_s)$
1.010	0.929	0.081	12.346
1.015	0.891	0.124	8.065
1.020	0.851	0.169	5.917
1.026	0.809	0.217	4.608
1.031	0.768	0.263	3.802
1.036	0.718	0.318	3.145
1.042	0.664	0.378	2.646
1.047	0.582	0.465	2.151

Table II (continued)

Summary of Dry Run Calculations (Probe)

	$(P_a - P_s)/P_a$	(P_o)	$(P_o)/(P_a - P_s)$
Run I-A	0.322	73.681	2.987
	0.276	74.028	3.508
Run I-B	0.303	72.846	3.176
	0.227	73.546	4.276
	0.160	74.154	6.103
Run I-C	0.344	73.226	2.784
	0.299	73.683	3.218
	0.260	74.019	3.720
	0.226	74.373	4.299
	0.175	74.742	5.578
Run I-D	0.284	74.399	3.400
	0.211	75.067	4.625
	0.229	74.920	4.252
	0.162	75.540	6.048
	0.193	75.303	5.061
Run I-E	0.105	74.732	9.377
	0.176	74.056	5.539
	0.284	72.986	3.392
	0.244	73.418	3.975
Run I-F	0.316	73.488	3.037
	0.248	74.089	3.899
	0.216	74.385	4.508
	0.174	74.757	5.621
	0.158	74.905	6.190

Appendix C-2

Table III

Summary of Probe Error Calculation for Normal Air

P_s/P_a	$(P_a-P_s)/P_a$	$(P_a-P_o)/(P_a)_T$	$(P_o/P_a)_T$	$(P_o/P_s)_T$
0.90	0.10	0.0124	0.9875	1.097
0.85	0.15	0.0182	0.9818	1.155
0.80	0.20	0.0237	0.9763	1.220
0.75	0.25	0.0294	0.9706	1.294
0.70	0.30	0.0344	0.9655	1.379
0.65	0.35	0.0390	0.9610	1.478

$(P_a-P_o)/(P_a)_P$	$(P_o/P_a)_P$	$(P_o/P_s)_P$	$\Delta P_o/P_s$	$(P_o/P_s)_T - 1$
0.0136	0.9864	1.096	0.001	0.097
0.0208	0.9792	1.152	0.003	0.155
0.0274	0.9726	1.216	0.004	0.220
0.0336	0.9664	1.289	0.005	0.294
0.0391	0.9609	1.373	0.006	0.379
0.0436	0.9564	1.471	0.007	0.478

$(100)(\Delta P_o/P_s)/\left[(P_o/P_s)_T - 1\right]$
1.03 %
1.94 %
1.82 %
1.70 %
1.58 %
1.46 %

Appendix C-3

Table IV

Summary of Primary Data Point Calculations

Test I - Dry Runs

		$(P_a-P_O)/(P_a)$	$(P_s)/(P_a)$
Probe #1	Run I-A	0.03704	0.67758
		0.03250	0.72424
	Run I-B	0.03928	0.69746
		0.03004	0.77316
		0.02202	0.83976
	Run I-C	0.04292	0.65625
		0.03695	0.70069
		0.03256	0.73990
		0.02793	0.77389
		0.02311	0.82486
	Run I-D	0.03347	0.71582
		0.02479	0.78922
		0.02670	0.77116
		0.01864	0.83780
		0.02172	0.80676
Probe #2	Run I-E	0.01440	0.89489
		0.02332	0.82367
		0.03743	0.71618
		0.03173	0.75641
	Run I-F	0.03950	0.68370
		0.03164	0.75167
		0.02777	0.78434
		0.02291	0.82617
		0.02098	0.84135

Table IV (continued)

Summary of Primary Data Point Calculations

Test II - 0.100 lbs/sec water

$(P_a/P_s) = 0.8103$

		(P_s) cm Hg	(P_a-P_s) cm Hg	(P_a-P_0) cm Hg	(P_0) cm Hg	(P_0/P_s)
Probe #1	Run II-A	61.794	14.467	4.062	72.199	1.1684
	Run II-B	62.564	14.647	4.012	73.199	1.1700
	Run II-C	61.996	14.514	4.040	72.470	1.1689
	Run II-D	62.373	14.602	3.992	72.983	1.1701
Probe #2	Run II-E	61.996	14.514	4.052	72.458	1.1688

Test III - 0.125 lbs/sec water

$(P_a/P_s) = 0.7337$

		(P_s) cm Hg	(P_a-P_s) cm Hg	(P_a-P_0) cm Hg	(P_0) cm Hg	(P_0/P_s)
Probe #1	Run III-A	56.691	20.576	6.078	71.189	1.2557
	Run III-B	56.646	20.560	6.180	71.026	1.2539
	Run III-C	56.342	20.450	6.380	70.412	1.2497
	Run III-D	56.143	20.377	6.180	70.340	1.2529
	Run III-E	56.477	20.498	6.022	70.953	1.2563
Probe #2	Run III-F	56.143	20.377	6.245	70.275	1.2517

Table IV (continued)

Summary of Primary Data Point Calculations

Test IV - 0.150 lbs/sec water

$(P_a/P_s) = 0.6482$

		(P_s) cm Hg	(P_a-P_s) cm Hg	(P_a-P_0) cm Hg	(P_0) cm Hg	(P_0/P_s)
Probe #1	Run IV-A	49.462	26.845	8.813	67.489	1.3645
	Run IV-B	50.078	27.179	8.712	68.545	1.3688
	Run IV-C	49.788	27.022	9.025	67.785	1.3615
	Run IV-D	49.686	26.966	8.511	68.141	1.3714
	Run IV-E	49.146	26.673	8.576	67.243	1.3682
	Run IV-F	49.600	26.920	8.791	67.729	1.3655
	Run IV-G	49.895	27.080	8.590	68.385	1.3706
Probe #2	Run IV-H	49.146	26.673	8.585	67.234	1.3680
	Run IV-I	49.600	26.920	8.779	67.741	1.3657

Test V - 0.100 lbs/sec water

$(P_a/P_s) = 0.59895$

		(P_s) cm Hg	(P_a-P_s) cm Hg	(P_a-P_0) cm Hg	(P_0) cm Hg	(P_0/P_s)
Probe #1	Run V-A	46.279	30.988	7.646	69.621	1.5044
	Run V-B	45.826	30.684	7.840	68.670	1.4985
	Run V-C	46.147	30.328	7.737	69.238	1.5004
Probe #2	Run V-D	45.826	30.684	7.850	68.660	1.4983

Appendix C-4

Table V

Summary of Modified Data Point Calculations

Test II - 0.100 lbs/sec water (injected)

$M_I = 0.382$ $\quad$ $M_I^2 = 0.1459$

$M_L = 0.476$ $\quad$ $M_L^2 = 0.2266$

$$\overline{M^2} = 0.1862$$

$$\frac{k\overline{M^2}}{2} = 0.13034$$

Date	$\Delta(\omega_w/\omega_a)$	ΔT_{02}	$(\Delta T_{02}/530)$	$(1-\frac{\Delta T_{02}}{530})$	$(1-\frac{\Delta T_{02}}{530})^{\frac{k\overline{M^2}}{2}}$	(P_0/P_s)orig	(P_0/P_s)mod
5/14	-0.0013	- 5.71	-0.01077	1.01077	1.00140	1.1701	1.1717
4/21	-0.0038	-16.68	-0.03147	1.03147	1.00410	1.1700	1.1748
5/7	-0.0017	- 7.46	-0.01408	1.01408	1.00184	1.1689	1.1711
5/7	-0.0017	- 7.46	-0.01408	1.01408	1.00184	1.1688	1.1710
4/13	0.0000	0.00	0.00000	1.00000	1.00000	1.1684	1.1684

Test III - 0.125 lbs/sec water (injected)

$M_I = 0.440$ $\quad$ $M_I^2 = 0.1936$

$M_L = 0.577$ $\quad$ $M_L^2 = 0.3329$

$$\overline{M^2} = 0.2632$$

$$\frac{k\overline{M^2}}{2} = 0.18424$$

Date	$\Delta(\omega_w/\omega_a)$	ΔT_{02}	$(\Delta T_{02}/530)$	$(1-\frac{\Delta T_{02}}{530})$	$(1-\frac{\Delta T_{02}}{530})^{\frac{k\overline{M^2}}{2}}$	(P_0/P_s)orig	(P_0/P_s)mod
5/14	0.0044	19.32	0.0365	0.9635	0.9932	1.2563	1.2478
4/21	0.0026	11.42	0.0215	0.9785	0.9960	1.2557	1.2507
4/21	0.0026	11.42	0.0215	0.9785	0.9960	1.2539	1.2489
5/7	0.0040	17.57	0.0332	0.9668	0.9938	1.2529	1.2451
5/7	0.0040	17.57	0.0332	0.9668	0.9938	1.2517	1.2439
4/23	0.0000	0.00	0.0000	1.0000	1.0000	1.2497	1.2497

Table V (continued)

Summary of Modified Data Point Calculations

Test IV - 0.150 lbs/sec water (injected)

$M_I = 0.480$ $M_I^2 = 0.2304$

$M_I = 0.678$ $M_I^2 = 0.4597$

$$\overline{M^2} = 0.3451$$

$$\frac{k\overline{M^2}}{2} = 0.24164$$

Date	$\Delta(\omega_w/\omega_a)$	ΔT_{02}	$(\Delta T_{02}/530)$	$(1-\frac{\Delta T_{02}}{530})$	$(1-\frac{\Delta T_{02}}{530})^{\frac{k\overline{M^2}}{2}}$	(P_0/P_s)orig	(P_0/P_s)mod
4/29	0.0064	28.12	0.0531	0.9469	0.9869	1.3714	1.3534
5/14	0.0044	19.32	0.0365	0.9635	0.9911	1.3706	1.3584
4/21	0.0026	11.40	0.0215	0.9785	0.9948	1.3688	1.3617
5/5	0.0050	21.97	0.0415	0.9585	0.9898	1.3682	1.3542
5/5	0.0050	*21.97	0.0415	0.9585	0.9898	1.3680	1.3540
5/7	0.0040	17.57	0.0332	0.9668	0.9919	1.3657	1.3546
5/7	0.0040	17.57	0.0332	0.9668	0.9919	1.3655	1.3544
4/14	0.0040	17.57	0.0332	0.9668	0.9919	1.3645	1.3534
4/23	0.0000	0.00	0.0000	1.0000	1.0000	1.3615	1.3615

Test V - 0.100 lbs/sec water (injected)

$M_I = 0.523$ $M_I^2 = 0.2735$

$M_I = 0.785$ $M_I^2 = 0.6162$

$$\overline{M^2} = 0.4448$$

$$\frac{k\overline{M^2}}{2} = 0.31136$$

Date	$\Delta(\omega_w/\omega_a)$	ΔT_{02}	$(\Delta T_{02}/530)$	$(1-\frac{\Delta T_{02}}{530})$	$(1-\frac{\Delta T_{02}}{530})^{\frac{k\overline{M^2}}{2}}$	(P_0/P_s)orig	(P_0/P_s)mod
4/21	-0.0014	-6.15	-0.01160	1.00160	1.00050	1.5044	1.5052
5/14	0.0004	1.76	0.00332	0.99668	0.9990	1.5004	1.4989
5/7	0.0000	0.00	0.00000	1.00000	1.00000	1.4985	1.4985
5/7	0.0000	0.00	0.00000	1.00000	1.00000	1.4983	1.4983

Appendix D

Table VI

Original Data

Test I - Dry Runs

			P_a(inches Hg)	(P_a-P_s)cm Hg	(P_a-P_o)in H_2O
Probe #1	Run I-A	4/13/54	30.124	24.67	38.40
				21.10	33.70
	Run I-B	5/5/54	29.852	22.94	40.35
				17.20	30.87
				12.15	22.63
	Run I-C	5/7/54	30.122	26.30	44.50
				22.90	38.30
				19.90	33.75
				17.30	28.95
				13.40	23.95
	Run I-D	5/14/54	30.305	21.80	34.90
				16.23	25.85
				17.62	27.85
				12.49	19.45
				14.38	22.65
Probe #2	Run* I-E	5/5/54	29.852	7.97	14.80
				13.37	23.95
				21.52	38.45
				18.47	32.60
	Run I-F	5/7/54	30.122	24.20	40.95
				19.00	32.50
				16.50	28.80
				13.30	23.75
				12.10	21.75

Table VI (continued)

Original Data

Test II - 0.100 lbs/sec water

			P_a(inches Hg)	(P_a-P_s)cm Hg	(P_a-P_0)in H_2O
Probe #1	Run II-A	4/13/54	30.024	12.52	49.29
				14.37	54.67
				16.02	58.40
	Run II-B	4/21/54	30.398	14.71	55.05
				13.95	52.20
				12.92	49.15
	Run II-C	5/7/54	30.122	16.08	60.00
				15.12	56.75
				13.65	50.90
				12.74	49.50
				14.02	53.20
	Run II-D	5/14/54	30.305	17.04	62.00
				15.93	57.55
				14.50	53.45
				13.33	49.70
				14.05	52.40
Probe #2	Run II-E	5/7/54	30.122	14.96	56.35
				12.41	49.75
				13.38	52.45
				14.19	53.95
				15.37	57.50

Table VI (continued)

Original Data

Test III - 0.125 lbs/sec water

		P_a(inches Hg)	(P_a-P_s)cm Hg	(P_a-P_0)in H_2O
Probe #1	Run III-A 4/21/54	30.420	19.64	79.10
			21.22	84.55
			17.52	71.15
	Run III-B 4/21/54	30.396	18.73	77.10
			19.75	80.60
			21.13	87.05
	Run III-C 4/23/54	30.233	18.92	81.05
			21.30	89.14
			22.54	94.18
			19.30	81.75
			20.61	87.98
			19.73	83.42
			20.21	85.73
			20.92	88.85
			21.70	92.05
	Run III-D 5/7/54	30.126	19.26	78.55
			20.19	82.45
			20.99	86.10
			22.10	90.00
			20.72	85.10
	Run III-E 5/14/54	30.305	19.70	79.39
			21.27	84.65
			21.98	86.40
			20.55	81.01
			18.97	75.40
Probe #2	Run III-F 5/7/54	30.126	20.19	83.80
			20.74	85.55
			21.36	88.23
			22.05	90.65
			19.10	78.76

Table VI (continued)

Original Data

Test IV - 0.150 lbs/sec water

		P_a(inches Hg)	(P_a-P_s)cm Hg	(P_a-P_s)in H_2O
Probe #1	Run IV-A 4/14/54	30.042	29.35	130.43
			28.80	127.38
			26.95	121.47
			27.95	124.10
	Run IV-B 4/21/54	30.416	26.10	113.50
			27.35	119.50
			28.33	122.20
	Run IV-C 4/23/54	30.240	26.86	121.70
			28.05	126.10
			26.07	117.95
			26.44	120.00
			27.34	124.25
			28.11	127.10
			27.45	123.65
	Run IV-D 4/29/54	30.178	26.50	113.41
			28.04	120.05
			27.44	117.20
			27.00	115.80
			26.95	116.35
			29.39	125.55
			28.11	120.20
	Run IV-E 5/5/54	29.850	25.87	115.15
			27.15	117.95
			28.25	122.85
	Run IV-F 5/7/54	30.126	25.63	113.75
			26.60	115.50
			27.05	118.80
			28.02	122.05
			26.39	116.75
	Run IV-G 5/14/54	30.305	27.93	112.25
			28.75	121.80
			26.44	113.85
			25.40	109.65
			27.47	118.15
Probe #2	Run IV-H 5/5/54	29.850	28.05	121.90
			28.34	123.20
			24.86	111.30
	Run IV-I 5/7/54	30.126	29.47	124.75
			27.00	118.35
			26.10	116.05
			26.56	117.65
			27.49	121.35

Table VI (continued)

Original Data

Test V - 0.100 lbs/sec water

			P_a (inches Hg)	$(P_a - P_s)$ cm Hg.	$(P_a - P_o)$ in H_2O
Probe #1	Run V-A	4/21/54	30.420	28.75	97.50
				26.43	91.10
				25.49	88.60
				27.05	94.40
	Run V-B	5/7/54	30.122	24.34	99.10
				28.75	101.30
				29.52	102.65
				30.08	104.10
				30.43	105.55
	Run V-C	5/14/54	30.305	26.83	93.60
				28.30	98.00
				29.23	101.50
				30.10	102.70
				28.90	99.50
Probe #2	Run V-D	5/7/54	30.122	30.15	105.35
				28.67	99.75
				27.43	95.80
				29.39	102.75
				30.55	107.30

Table VI (continued)

Original Data

Date	Specific humidity (lbs water/lbs air)
4/13/54	0.0045
4/14/54	0.0062
4/21/54	0.0083, 0.0076
4/23/54	0.0102
4/29/54	0.0038
5/5/54	0.0052
5/7/54	0.0062
5/14/54	0.0058

Appendix E

Literature Citations

1. Shapiro, A.H. and Hawthorne, W.R., "The Mechanics and Thermodynamics of Steady, One-Dimensional Gas Flow," Journal of Applied Mechanics, December 1947, pp A-317 to A-336.

2. Gavril, B.D., "A Theoretical Investigation of the Thermodynamic and Dynamic Effects of Water Injection into High-Velocity, High-Temperature Gas Streams," Thesis for degree of Doctor of Science, M.I.T., in preparation.

3. Dussourd, J.L., "Instrumentation For An Air Stream Carrying Water Droplets," Thesis for degree of Doctor of Science, M.I.T. in preparation.

4. Wadleigh, K.R., "An Experimental Investigation of a Small-Scale Aerothermopressor - A Device for Increasing The Stagnation Pressure of a High-Temperature, High-Velocity Gas Stream by Evaporative Cooling," Thesis for degree of Doctor of Science, M.I.T., 1953.

5. Hoerner, S.F., "Aerodynamic Drag," Otterbein Press, Dayton, Ohio 1951.

6. Keenan, J.H. and Kaye, J., "Gas Tables", John Wiley & Sons, New York 1945.

7. Shapiro, A.H., "The Dynamics and Thermodynamics of Compressible Fluid Flow," Ronald Press Co., New York 1953, pp.231.

8. "Steels For Elevated Temperature Service," Carnegie-Illinois Steel Corporation, Pittsburgh and Chicago 1949, pp.61.

9. "Energy Analysis of Naval Machinery," United States Naval Institute, Annapolis, 1940, pp. 23-12.

Thesis
C267

28814

Carpenter

Construction and preliminary test of a traversing stagnation pressure probe for a large scale aerothermopressor.

28814

C267

Carpenter

Construction and preliminary test of a traversing stagnation pressure probe for a large scale aerothermopressor.

thesC267
Construction and preliminary test of a t
3 2768 002 08565 6
DUDLEY KNOX LIBRARY